# Interactions of amyloid coaggregates with biomolecules and its relevance to neurodegeneration

AUTHOR(S):

Murakami, Kazuma; Ono, Kenjiro

CITATION:

Murakami, Kazuma ...[et al]. Interactions of amyloid coaggregates with biomolecules and its relevance to neurodegeneration. The FASEB Journal 2022, 36(9): e22493.

ISSUE DATE:

2022-09

URL:

http://hdl.handle.net/2433/276801

# Interactions of amyloid coaggregates with biomolecules and its relevance to neurodegeneration

Kazuma Murakami[a,*] and Kenjiro Ono[b,*]

[a]Division of Food Science and Biotechnology, Graduate School of Agriculture, Kyoto University, Kyoto, Japan
[b]Department of Neurology, Kanazawa University Graduate School of Medical Sciences, Kanazawa, Japan

*Corresponding authors
Kazuma Murakami: murakami.kazuma.4v@kyoto-u.ac.jp
Kenjiro Ono: onoken@med.kanazawa-u.ac.jp

**Authors' information**
ORCiD 0000-0003-3152-1784 (K.M.)
ORCiD 0000-0001-8454-6155 (K.O.)

**Abstract**

The aggregation of amyloidogenic proteins is a pathological hallmark of various neurodegenerative diseases, including Alzheimer's disease, Parkinson's disease, and amyotrophic lateral sclerosis. In these diseases, oligomeric intermediates or toxic aggregates of amyloids cause neuronal damage and degeneration. Despite the substantial effort made over recent decades to implement therapeutic interventions, these neurodegenerative diseases are not yet understood at the molecular level. In many cases, multiple disease-causing amyloids overlap in a sole pathological feature or a sole disease-causing amyloid represents multiple pathological features. Various amyloid pathologies can coexist in the same brain with or without clinical presentation and may even occur in individuals without disease. From sparse data, speculation has arisen regarding the coaggregation of amyloids with disparate amyloid species and other biomolecules, which are the same characteristics that make diagnostics and drug development challenging. However, advances in research related to biomolecular condensates and structural analysis have been used to overcome some of these challenges. Considering the development of these resources and techniques, herein we review the cross-seeding of amyloidosis, e.g., involving the amyloids amyloid β, tau, α-synuclein, and human islet amyloid polypeptide, and their cross-inhibition by transthyretin and BRICHOS. The interplay of nucleic acid-binding proteins, such as prions, TAR DNA-binding protein 43, fused in sarcoma/translated in liposarcoma, and fragile X mental retardation polyglycine, with nucleic acids in the pathology of neurodegeneration are also described, and we thereby highlight potential clinical applications in central nervous system therapy.

**Keywords:** amyloid, coaggregation, neurodegenerative disease, oligomer, DNA, RNA, nucleic acid-binding protein, G-quadruplex

## Introduction

Neurodegenerative diseases are characterized by the progressive degeneration of the neuronal system. Many of these diseases are age-related, as exemplified by Alzheimer's disease (AD) and other tauopathies, Parkinson's disease and other synucleinopathies, prion diseases, and other sporadic or genetic proteinopathies. Aggregation of amyloidogenic proteins, such as amyloid β (Aβ), tau, α-synuclein (αSyn), prion protein, transactive response DNA-binding protein 43 (TDP-43), and fused in sarcoma/translated in liposarcoma (FUS/TLS), is thought to be a cause or a major deleterious result in most cases of these diseases. Such disease-related amyloids are prone to self-assembly into matured amyloid fibrils (1). In some neurodegenerations, oligomers, which have structurally metastable intermediates in a wide range of molecular sizes, commonly serve as neuronal toxins rather than the structurally stable fibrils. Oligomeropathy is responsible for the molecular pathogenesis of the associated diseases (2-5) and causes impaired synaptic function and neuronal death through oxidative stress, inflammation, apoptosis, and dysfunction of proteostasis (6). Thus, oligomers have gained attention as targets for research and drug development related to diagnostics and therapeutics.

In relation to amyloid assembly, "oligomer" is an ambiguously defined term used to describe dimers as well as hundreds of monomers when they are water-soluble, which further complicates drug targeting (7-9). Despite, over recent decades, substantial research effort directed at therapeutic interventions, there is no cure for oligomeric assembly as a therapy for neurodegeneration, which has two possible explanations as follows. (1) Reversible equilibrium: the formation of toxic oligomers resistant to degradation occurs, whereas the self-assembly process redirects toward dissociation back to nontoxic monomers. These properties increase the difficulty involved in targeting specific dimensions of oligomers. (2) Nonuniformity: the mechanism of amyloid propagation is generally explained using a uniform stacking model, as represented by a nucleation-dependent polymerization model (10) or a template-dependent dock–lock model (11); however, most neurodegenerative diseases show overlapping clinical symptoms, e.g., among AD, tauopathies, and synucleinopathies (12-14). Concomitantly, coaggregation or co-oligomerization of amyloids occurs in the brains of patients (15, 16). In addition, other biomolecules, such as nucleic acids (e.g., total RNA and noncoding RNA) (17, 18), interact with aggregates as cofactors and have been characterized as inducers of further unsettled co-oligomerization. Due to these two characteristics, the epidemiology, diagnosis, and treatment of mixed dementia remains complex and challenging.

Structural analysis is a powerful approach used to achieve molecular understanding and drug development related to amyloidosis. The analysis of biomolecules under conditions that imitate biological environments within cells or tissues has attracted the attention of researchers. For example, Tycko and colleagues have pioneered research in this challenging field using solid-state nuclear magnetic resonance (ssNMR) and were the first to represent *ex vivo* structures of amyloid β40 (Aβ40) (19) from AD brain tissue, comprising two or three identical filaments with a C-shaped fold and right-handed twist. Compared with the *in vitro* structure of Aβ40 fibrils (20), the monomer units resemble each other, but several differences exist at the single-residue level between *ex vivo* and *in vitro* Aβ40 fibril structures in the side-chain

orientation and the contact mode in interfilament packing. Subsequently, Tycko's group analyzed the *ex vivo* structures of amyloid β42 (Aβ42) (21), its more aggregative isoform, in variable AD clinical subtypes. Although the structure of Aβ42 fibrils largely differs from that of Aβ40 fibrils and has structural heterogeneity with at least two prevalent structures in most patients, detailed structural modeling of Aβ42 fibrils was not presented. In prior studies, three independent groups reported the *in vitro* structures of Aβ42 fibrils (22-24) based on ssNMR experiments, with results indicating an S-shaped conformation with a right-handed twist in the middle and C-terminal regions, in addition to a disordered region at the N-terminal region. The salt bridge between Lys28 and the carbonyl group of the C-terminus could be involved in stabilization of the fibril structure. Given the structural difference between fibrils from Aβ40 and Aβ42, the coaggregation of Aβ40 with the seed of Aβ42 fibrils did not occur (22).

Structural analysis of *ex vivo* Aβ fibrils from post mortem human AD brains has been expanded to include cryogenic electron microscopy (cryo-EM). In 2019, Fändrich and colleagues demonstrated that an *ex vivo* Aβ40 fibril fold purified from AD brain tissue was C-shaped with a right-hand twisted, in which its N- and C-terminal ends formed arches (25). These structures differed from that of the *in vitro* Aβ40 fibril (26, 27), a structure that was also proposed by Fändrich's group using cryo-EM. Ultimately, Yang et al. succeeded in clarifying *ex vivo* Aβ42 fibrils from the brains of patients with AD (28), showing two types of S-shaped filaments, including a N-terminal region around Y10 and V12 and a turn position that slightly shifted accordingly as well as a salt bridge formation between Lys 16 and Glu22 that was more contributable compared with that between Lys 28 and the carbonyl group of the C-terminus. Moreover, the participation of the N-terminal region to the S-shaped domain was not implied in the structures of *in vitro* Aβ42 fibrils based on ssNMR (22-24) (**Fig. 1a**). These differences between *ex vivo* and *in vitro* results suggested that biomolecular cofactors were required for the formation of amyloid fibrils in brains with AD pathology. *Ex vivo* cryo-EM analyses have also been applied to other neurodegeneration-associated amyloid fibrils (e.g., tau (29) and TDP-43 (30)). As observed in comparisons of Aβ40 and Aβ42, the structures of *in vitro* tau filaments by X-ray diffraction and Fourier transform infrared spectroscopy (31) do not reflect those of *ex vivo* tau filaments derived from patients with AD (29) (**Fig. 1b**). Moreover, *ex vivo* TDP-43 filaments (30) have a double spiral-shaped fold in their low-complexity domain, including turns and β-strands composed of glycine and neutral polar residues, which shows little similarity to that of *in vitro* TDP-43 filaments (32, 33) (**Fig. 1c**). Despite the recognition that coaggregation is important in neurodegeneration, structural determination of coaggregates reflecting their biological environment and formation process has not been achieved.

When attempting to overcome the chaotic state in metastable protein assemblies in the brain, approaches in which molecular dynamic analysis is focused on biomolecular condensates and technology advancements in NMR and cryo-EM could be useful if the coaggregating molecules are localized and condensed in small organelles. In this review, we provide an update on the mechanistic insights into coaggregation (or cross-seeding) of neurodegeneration-related proteins with a focus on Aβ, tau, αSyn, prions, TDP-43, and FUS/TLS, the molecular sizes of which range across an order of magnitude 40–520-mer residues. The interplay with RNA, which

functions as an amyloid trapping molecule in the misplacement of encoding messages and thereby induces cellular deterioration, is an emerging “hot topic” in the proteinopathy research field, as exemplified by nucleic acid-binding proteins (e.g., prions, TDP-43, and FUS/TLS) and fragile X mental retardation polyglycine (FMRpolyG). The application of each amyloid coaggregation with different amyloid species or biomolecular cofactors has been separately reviewed in the past; however, to our knowledge, there has been no comprehensive review of amyloid coaggregates from the perspective of their interaction with cytosolic or nuclear biomolecules and potential overlap among neurodegenerative diseases. In this review, we also discuss how these coaggregates could play supramolecular roles in potential strategies for discovery of central nervous system (CNS)-targeting drugs and the development of therapeutics for neurodegeneration.

## Disparate amyloid cross-seeding and cross-inhibition in neurodegeneration

Neurodegenerative diseases are characterized by aggregates of proteins such as Aβ, tau, and αSyn, the pathological forms of which appear to spread through the brain in characteristic patterns (34, 35). Although each disease exhibits the accumulation of specific characteristic protein aggregates, many cases exist in which aggregation of multiple pathological proteins is exhibited. Studies in *in vitro*, cellular, and *in vivo* systems have revealed several potential types of interactions between the different pathological proteins involved in neurodegeneration, including cross-seeding of aggregates in one protein initiating misaggregation of another. To explain the mechanisms of fibril formation of amyloidogenic proteins *in vitro*, a nucleation-dependent polymerization model has been used (10). This model consists of two phases: nucleation and seeding extension. Nucleus formation requires a series of association steps of monomeric proteins that are thermodynamically unfavorable, representing the rate-limiting step in fibril formation. Once the nucleus (seed) has been formed, the further addition of monomers becomes thermodynamically favorable, resulting in the seeding extension of fibrils. This model was originally advocated as a model for a single amyloid (Aβ) (10), but it has also been applied with a combination of different amyloids; accordingly, it is thought that various types of seeding aggregation can occur depending on the number of amyloids involved (**Fig. 2**). Below, we attempt to shed light on the amyloid proteins and their cross-seeding effects (**Table 1**) and occasionally cross-inhibition effects (**Table 2**).

### *Aβ cross-seedingwith tau aggregation*

AD is characterized by the accumulation of extracellular Aβ plaques and intracellular tau neurofibrillary tangles (NFTs) pathologically. It was found that Aβ binds to multiple tau peptides, especially those in exons 7 and 9, whereas tau binds to multiple Aβ peptides in the middle portion to C-terminal regions of Aβ (36). Such binding affinity between Aβ and tau was almost 1,000-fold higher than that of tau for itself. In P301L mutant tau transgenic mice, injection of Aβ42 fibrils can significantly accelerate NFT formation, which further induces the phosphorylation of tau (37), indicating that the cross-seeding interaction of Aβ42 with P301L tau generates many more NFTs than are generated by either Aβ42 or P301L tau alone. Similarly,

the introduction of tau in Tg2576 transgenic mice was found to enhance the expression of mutant Aβ precursor protein (APP) and subsequent aggregation of Aβ (38).

*Aβ cross-seeding with αSyn aggregation*

Up to 50% of AD cases exhibit significant Lewy bodies (LBs) pathology in addition to plaques and tangles (39, 40). Compared with pure AD, AD with LBs pathology as a secondary lesion has been reported with lower mini mental state examination scores and more advanced dementia, suggesting that the severity of the disease increases due to complications related to LBs pathology (41). Likewise, patients with dementia with LB (DLB) frequently exhibit AD pathology, particularly senile plaques (42). Autopsy studies of 213 patients with LBs disorder in which the burden of tau NFTs and neuritic plaques was assessed revealed 26% with low-level AD neuropathology, 21% with intermediate-level AD neuropathology, and 30% with high-level AD neuropathology (43). As levels of AD neuropathology increased, cerebral αSyn scores also increased, and the interval between onset of motor and dementia symptoms and disease duration was shorter. In the same study, multivariate regression revealed independent negative associations between the cerebral tau NFT score and the interval between onset of motor and dementia symptoms (43).

Using transgenic mice with neuronal expression of Aβ and αSyn, it was shown that Aβ enhances αSyn accumulation and neuronal deficits (44). An NMR study showed that Aβ and αSyn might interact directly at a few sites (45). Although various studies have identified Aβ and αSyn oligomers as central toxic events during AD and LBs disease, leading to cell death and synaptic dysfunction (3, 46), a specific *in vitro* study found that Aβ and αSyn might interact directly to form hybrid pore-like oligomers that contribute to neurodegeneration (47). Previously, Ono and colleagues showed that fibrils and oligomers of Aβ40, Aβ42, and αSyn acted as seeds and affected the aggregation pathways within and among species *in vitro* (48). The seeding effects of αSyn fibrils were increased relative to those of Aβ40 and Aβ42 fibrils in the Aβ40 and Aβ42 aggregation pathways, respectively. It was also shown that Aβ and αSyn acted as seeds and each affected the aggregation pathway of the other *in vitro* (48).

*Tau cross-seeding with αSyn aggregation*

Lee's group found that one strain of preformed αSyn fibrils can be directly cross-seeded for tau aggregation, both in neuron cultures and an *in vivo* model of tau (49). This group injected αSyn preformed fibrils into mice with abundant Aβ plaques, and the Aβ deposits dramatically accelerated αSyn pathogenesis and spread throughout the brain. Remarkably, phosphorylated tau was induced in αSyn fibril-injected 5×FAD mice, and these mice showed neuron loss that was correlated with the progressive decline of cognitive and motor performance. These findings suggest the existence of a feed-forward mechanism in which Aβ aggregates enhance endogenous αSyn aggregation and spreading, which exacerbates the pathogeneses of Aβ and tau temporally postinjection with preformed fibrillar seeds of αSyn (50).

*Aβ or αSyn cross-seeding with IAPP aggregation*

Islet amyloid polypeptide (IAPP) is an amyloidogenic protein secreted as a randomly unstructured peptide. It plays a vital role in the progression of type 2 diabetes (T2D) mellitus; indeed, autopsies of bodies with this disease displayed IAPP aggregates in the pancreatic islets (51). The conformation of IAPP is assumed to be changed from a random structure to β-sheets before aggregation (52). Several studies have shown that individuals with AD develop signs and symptoms of T2D or other glucose-related disorders, whereas individuals with T2D are at a higher risk than healthy individuals of developing AD (53, 54). A study on the interaction of Aβ and IAPP showed that IAPP promotes Aβ42 oligomerization and the formation of larger heteroaggregates with enhanced toxicity in neuronal cells (55). In the same study, Aβ42 and IAPP interacted to form heterocomplex aggregates, which induced cell death in neuroblastoma cells (55). In transgenic mice, an intravenous injection of preformed Aβ fibrils triggered IAPP aggregation in the pancreas, suggesting that Aβ could enhance IAPP aggregation through cross-seeding (56). Several studies have reported the presence of αSyn in pancreatic β cells (57, 58). One study showed that the octapeptide TKEQVTNV from αSyn can cross-seed with IAPP monomers and facilitate IAPP fibrillization (59). Contrary to expectations, this cross-seeding increased cell viability and reduced IAPP-induced cytotoxicity by shifting into a different seeding pathway of IAPP (59).

*TTR cross-inhibition with Aβ or IAPP aggregation*

Along with cross-seeding between discrete amyloidogenic proteins, there are smaller but respectable literatures on the cross-inhibition against fibrillogenesis in Aβ or IAPP by two other amyloids, i.e. TTR and BRICHOS. These amyloids are known as a paradox of amyloidogenic proteins with anti-amyloid aggregation properties, but the structural analysis using NMR and cryo-EM has not yet carried out. TTR is a 127-mer homotetrameric protein, which can be expressed mostly in the liver and be secreted into the plasma (60, 61). TTR molecules can misfold and form amyloid fibrils in the heart and peripheral nerves in the patients with TTR amyloidosis. The initial step in TTR aggregation is rate-limiting, and is involved in the dissociation of the native tetramer into monomers that subsequently undergo conformational changes forming aggregation-prone intermediates (60, 61).

Johnson and colleagues demonstrated that neutralization of TTR by chronic infusion of an anti-TTR antibody into the hippocampus of Tg2576 mice as a Aβ-overexpressing AD model exacerbates Aβ accumulation, tau phosphorylation, and neuronal loss (62). The same group reported that hemizygous deletion of TTR in APPswe/PS1ΔE9 mice resulted in earlier Aβ deposition in the cortex and hippocampus compared to control mice (63). These results suggest that TTR plays a critical role in the prevention of several AD pathologies. To explore the effect of TTR on Aβ aggregation, thioflavin-T (Th-T) fluorescence assay and TEM were carried out by Olofsson and colleagues (64). They demonstrated that TTR inhibited fibril formation primarily by interfering the nucleation stage, resulting in the formation of Th-T-negative non-amyloid aggregates. It is noteworthy that TTR did not affect the seeding extension process in Aβ aggregation (64). Further studies by Knowles and Chiti using atomic force microscopy (AFM) and dynamic light scattering (DLS) revealed that TTR inhibited both the primary and

secondary nucleation phases, but not fibril elongation, and then Aβ oligomers-induced cytotoxicity was reduced by TTR treatment (65).

TTR is expressed within the IAPP producing β-cells. Although there are no in vivo reports on cross-inhibition of IAPP aggregation by TTR, it was shown that TTR not only delayed the lag-phase but also impaired the elongation phase during the process of IAPP aggregation by Th-T assay (66). In addition, the interfering potential of TTR could be correlated inversely to thermodynamic stability, but no such correlation was observed in the dissociation rate of the tetramer (66). In AD model mice (*App*$^{NL\text{-}F/NL\text{-}F}$), high fat diet (HFD) treatment caused obesity and impaired glucose tolerance (i.e., T2D-like phenotypes), and an impaired cognitive function accompanied by marked increases in both Aβ deposition and microgliosis in the hippocampus were observed (67). Further to investigate, HFD treatment decreased TTR expression in *App*$^{NL\text{-}F/NL\text{-}F}$ mice, indicating that the depletion of TTR could underly the increased Aβ deposition in AD pathology (67). These results imply TTR as a potential target of disease treatment for AD and T2D.

*BRICHOS cross-inhibition with Aβ or IAPP aggregation*

BRICHOS is a 100-mer protein domain found in 12 protein families including over 300 proteins with a chaperon function (68). Especially, integral membrane protein 2B (ITM2B or Bri2) is a protein that in humans is encoded by the ITM2B gene, which is related to familial Danish dementia and familial British dementia, and Bri3 is a mutant of Bri2. BRICHOS domain from both Bri2 and Bri3 interacted with Aβ in neurons of AD patients (69). Studies on transgenic *Drosophila melanogaster* showed that co-expression of Aβ42 and BRICHOS domain in the brain delayed Aβ42 aggregation and significantly improved both lifespan and locomotor function compared with only Aβ42-expressing flies (70). Moreover, BRICHOS increased the ratio of soluble to insoluble Aβ42, and bound to Aβ aggregates (70), but the effects of each Bri2 or Bri3 were not studied in this study. In further studies using *Drosophila melanogaster* expressing Bri2 by the same group, the neurotoxic effects of Aβ42 were downregulated in the fly brains (71).

There have been several in vitro reports that prosurfactant protein C (proSP-C) BRICHOS and Bri2 BRICHOS significantly reduced the aggregation speed at substoichiometric levels by directly interacting with Aβ42. Bri2 BRICHOS also suppressed the formation of toxic Aβ42 oligomers by specifically preventing the secondary nucleation pathway to remove the dominant source of Aβ42 oligomers (72). 3D reconstruction of Bri2 BRICHOS analysis using TEM revealed that the monomers of Bri2 potently prevented Aβ42-induced cytotoxicity. In particular, the dimers strongly suppressed Aβ42 fibril formation by assembling into high molecular weight oligomers with a two-fold symmetry and the oligomers inhibited non-fibrillar aggregation. These data imply that Bri2 BRICHOS could harbor the molecular chaperone diversity by forming quaternary structures (73). As a comparison study, Bri3 BRICHOS also inhibited Aβ fibrillization and non-fibrillar protein aggregation in vitro by forming high molecular weight oligomers although the inhibitory effect of BRICHOS from Bri3 was weaker compared to that of Bri2 (74), raising a possibility of different roles for Bri2 and Bri3 BRICHOS against Aβ

pathology.

Regarding the cross-inhibition with IAPP, the effects of BRICHOS on IAPP aggregation and toxicity have been explored using in vitro studies, fly studies, and T2D patient materials (75). The BRICHOS domain of Bri2 intracellularly colocalized with IAPP in amyloid deposits of T2D patients. Bri2 BRICHOS showed a strong inhibitory activity against IAPP aggregation through targeting the secondary nucleation and redirecting the reaction towards formation of amorphous aggregates. Moreover, IAPP-induced toxicity was exacerbated in the human β-cell line EndoC-βH1 whose endogenous expression of Bri2 was downregulated by siRNA, whereas a concomitant overexpression of Bri2 BRICHOS recovered the cell viability. Similarly, the coexpression of IAPP and Bri2 BRICHOS in lateral ventral neurons of a Drosophila model increased the survival rate (75). These findings suggest that BRICHOS can be a potential endogenous inhibitor of IAPP pathologies, and then can be important therapeutic target T2D as well as AD.

**Coaggregation of amyloidogenic proteins with nucleic acids in neurodegeneration**

In 1998, a study on the detection of cytoplasmic RNAs in the pathological lesions of diverse neurodegenerative diseases was reported (76). Two pathological characteristics of AD, senile plaques and neurofibrillary tangles, contain RNA (77, 78). Mammalian nucleic acids have also been studied as cofactors for aggregation of several amyloidogenic proteins in proteinopathies. RNA and DNA molecules are postulated to interact with amyloids either directly or indirectly, resulting in conformational conversion, misfolding, aggregation, and infection. Inherently, most amyloids bind to polyanions, such as nucleic acids, glycosaminoglycans, and lipids (79-81). It was assumed that amyloid aggregates and nucleic acids would act as polyelectrolytes based on electrostatic forces (82). Each DNA or RNA has specific advantages and limitations in terms of chemical properties and structure, which are determined by Watson–Crick-type and Hoogsteen-type base pairings. Faced with enzymatic degradation, DNA oligonucleotides are more stable than their RNA counterparts. In contrast, the presence of the 2′-OH in ribose, as opposed to deoxyribose, potentially enables the higher conformational stability and diversity of RNA (83) (**Fig. 3a**). The absence of the 5′-methyl group in uracil, in contrast to its presence in thymine, has a similar impact on RNA properties. Indeed, nucleic acid (i.e., RNA and DNA) aptamers acting as synthetic oligonucleotides targeting Aβ, tau, αSyn, and prions have been extensively investigated as a means of disturbing the interaction of amyloids with nucleic acids (reviewed by Murakami et al. (9)). In comparison, studies of coaggregation of amyloids with endogenous nucleic acids causing pathologies have concentrated primarily on four examples of nucleic acid-binding proteins, i.e., prions, TDP-43, FUS/TLS, and FMRpolyG; therefore, these proteins are the focus of the subsections that follow. The binding characteristics of amyloidogenic proteins and nucleic acids and the subsequent nucleic acid-binding amyloids included in this review are summarized in **Table 3**.

*Prion coaggregation with DNA or RNA*

Human and animal prion diseases, including Creutzfeldt–Jakob disease, Kuru, Gerstmann–

Sträussler–Scheinker disease, and fatal familial insomnia in humans, bovine spongiform encephalopathy in cattle, scrapie in sheep and goats, and chronic wasting disease in deer and elk (84-86), are characterized by aberrant accumulation of misfolded prion protein (PrP). PrP consists of 253 amino acids and contains RNA recognition motif (RRM) and glycine rich domain (GXXXG) (87) (**Fig. 4a**). PrP exists physiologically as $PrP^{C}$ (cellular form), which functions in neuroprotection and trophic signaling, whereas $PrP^{C}$ can misfold into a toxic conformation as $PrP^{Sc}$ (scrapie form) due to genetic and environmental causes (88, 89). $PrP^{Sc}$ can form various conformational strains that are self-propagating and transmissible from cell to cell. The infectivity of $PrP^{Sc}$ within the same species and sometimes across species is contingent on the specific strain and strain barrier. $PrP^{C}$ is normally rich in α-helixes, yet $PrP^{Sc}$ forms a cross-β structure of amyloid fibrils upon aggregation due to some cofactors and acquires resistance to proteinases and denaturing, which leads to neurotoxicity (90). Thus, conversion of $PrP^{C}$ to $PrP^{Sc}$ or aggregation of $PrP^{Sc}$ is a potential therapeutic target for the development of drug modalities.

Nucleic acids have attracted attention as key physiological factors required for the transformation of $PrP^{C}$ to $PrP^{Sc}$. In 1997, Nandi first identified a bovine papilloma virus-derived plasmid DNA (16 kb) as a nucleic acid binder of PrP, showing that it bound to human PrP106-126 to possibly induce its structural change (91). A subsequent study by the same group revealed that human PrP106-126 generated amyloid fibrils with the addition of plasmid DNA but not without such DNA (92), suggesting that DNA plays a role as a cofactor in prion aggregation. For murine PrP23-231, a longer isoform, this was also the case in terms of its coaggregation with DNA (93), implying that nucleic acid metabolism is modulated by PrP.

Cordeiro et al. demonstrated the relevance of DNA to the pathology of prion-related diseases (94), finding, via circular dichroism (CD) spectrometry analysis, that the double-stranded DNA (18–34 bp; e.g., *recA1/2, Lexcons24, Lexcons 28,* and *E2DBS*) in molar excess (>2:1) over prions transformed murine PrP23-231 (i.e., $PrP^{C}$) to $PrP^{Sc}$ and triggered the aggregation of $PrP^{Sc}$ to induce fibril formation in a light-scattering assay. In contrast, the aggregation of Syrian hamster PrP109-141 and PrP109-149 was prevented by the presence of an equal or lower molar level of DNA oligonucleotides. A further study by this group showed that artificial single-stranded DNA oligonucleotides (18 or 21 nt in length) with different GC contents enhanced the aggregation of murine PrP23-231 in a light-scattering assay and transmission electron microscopy (TEM) as well as inducing the neurotoxicity of murine PrP23-231 in murine neuroblastoma cells (Neuro-2a cells) in a MTT test and caspase release assay (95). These findings indicate that the abundance of cellular DNA can contribute to PrP misfolding and neuronal death by modulating the equilibrium between $PrP^{Sc}$ and $PrP^{C}$ in neurodegeneration, and the possible interaction between DNA and PrP might originate from GC sequences. The dependency of prion–DNA binding on GC content is consistent with the preferable binding of small-length DNA aptamers (12-mer) that form the G-quadruplex, a noncanonical structure of nucleic acids induced via Hoogsteen-type base pairing, to ovine PrP23-231 (96). The G-quadruplex structure includes a stable planar core comprising four guanine bases in the same plane that form G-tetrads with Hoogsteen-type base pairing (**Fig. 3b**)

(97). G-quadruplex formation is involved in the protein–nucleic acid association through π–π interactions. The studies conducted to date suggest that endogenous DNA may facilitate prion propagation and aggregation by acting as a scaffold or molecular glue through the interaction between $PrP^{C}$ and $PrP^{Sc}$. We propose that excess nucleic acids might modulate the balance between physiological PrP and misfolded PrP by making protein–protein interactions more likely.

Structural insights into the recognition of DNA oligonucleotides by mouse PrP23-231 have been provided using NMR and small-angle X-ray spectroscopy (SAXS) (98). SAXS is a small-angle scattering technique that can be used to determine the dynamics and structural information of molecules via analysis of the elastic scattering mode of X-rays at small angles. The SAXS data confirmed that mouse PrP23-231 forms a complex with 18-bp DNA in which the globular domain of C-terminal PrP, rather than the disordered region in the N-terminal portion, might contribute to complex formation (98). Perturbation experiments of the chemical shift in $^{15}N$-$^{1}H$ HSQC NMR using $^{15}N$-labeled Syrian hamster PrP90-231 suggested that α-helix structures in the C-terminal region of PrP could be involved in the association with DNA (98).

In contrast to smaller length single-stranded DNA (i.e., <50 bp), longer length single-stranded RNA (several hundreds of nucleotides) plays a role in binding to PrP, which has RNA binding and chaperoning activities in relation to nucleocapsid retroviral proteins, such as NCp7 of human immunodeficiency virus (HIV) type 1. HIV-derived RNA has some resistance to proteinase K digestion through the formation of a complex with PrP, leading to PrP aggregation (99). According to NMR measurements using the N-terminal truncated peptide of PrP, the N-terminal region could participate in RNA binding in a similar manner to DNA. Additionally, RNA sources from mammals, yeast, or bacteria induced the aggregation of mouse PrP. Furthermore, PrP23-231 aggregated by incubation with total RNA from mouse neuroblastoma cells (Neuro-2a cells) was cytotoxic to such cells, and this cytotoxicity was consistent with the conformational change from an α-helix to β-sheet according to CD spectrometry analysis (99). The conversion of $PrP^{C}$ to $PrP^{Sc}$ was also stimulated by total RNA isolated from the hamster brain (100). Based on an *in vitro* conversion assay following the protein-misfolding cyclic amplification method and using prion-infected brain homogenate as a propagation seed, Saborio et al. demonstrated that RNA can be a requisite for the conversion and accumulation of pathogenic $PrP^{Sc}$ (101). In this method, amplification is based on multiple cycles of $PrP^{Sc}$ incubation in the presence of excess $PrP^{C}$ followed by sonication. During the incubation periods, further $PrP^{Sc}$ aggregation occurs through the incorporation of $PrP^{C}$, whereas the aggregates dispersed by sonication expand the population of converting units. Recently, the G-quadruplex formation of $PrP^{C}$ mRNA was implied as the missing link in the initial conversion of $PrP^{C}$ to $PrP^{Sc}$ (102), suggesting that G-quadruplex binders or inhibitors could be therapeutics for prionoid diseases. Pseudoknot, a functional nucleic acid structure that contain stem-loop structures through Watson-Crick interaction and Hoogsteen interaction (103) (**Fig. 3c**), was reported to function as a recognition motif with human $PrP^{C}$ similar to that of tRNA (104). These RNA structures can form stable nucleoprotein complex with human prion proteins.

Whether the PrP–RNA interaction occurs as a pathological trigger has not been shown

conclusively *in vivo*. $PrP^C$ is localized physiologically at the plasmatic membrane, whereas misfolded $PrP^C$ is believed to translocate to the nucleus of neuronal and endocrine cells where it interacts with chromatin (105, 106). It has been speculated that abnormal nuclear compartmentalization of $PrP^C$ causes prion pathogenesis through encounters with RNA counterparts. Alternatively, crosstalk between $PrP^C$ and RNA might be possible in the endocytic pathway because exogenous PrP binds endocytotically to nucleic acid. The endosomal recycling compartment was also identified as the likely site of the structural conversion of $PrP^C$ (107). Indeed, cytosolic $PrP^C$ was shown to form various RNA granule forms derived from nuclear RNA, 5S ribosomal RNA, or total RNA in Neuro-2a cells (108). Other studies reported that the $PrP^C$ to $PrP^{Sc}$ conversion occurred on the plasma membrane following the infection of the host with scrapie from external sources (109, 110). Collectively, the plasmatic membrane, nuclear compartment, cytosol, and plasma membrane can be considered crosstalk locations.

As mentioned above, experimental evidence has been accumulated on PrP–nucleic acids interactions, $PrP^C$ to $PrP^{Sc}$ conversion catalysts, and the induction of cytotoxicity. Sometimes, the coaggregation of prions can be accelerated by additional cofactors, such as copper. Indeed, $PrP^C$ is a copper-binding protein with superoxide dismutase activity, whereas $PrP^{Sc}$ is dependent on its copper-binding capacity (111, 112). One study found that the association of $CuCl_2$ in the interaction between ovine $PrP^C$ and total RNA was fundamental for structural conversion to β-sheet-rich $PrP^{Sc}$ and the acquisition of resistance to proteinase K (113). More studies on this relationship will be required to facilitate the development of antiprion drugs.

*TDP-43 coaggregation with RNA*

The DNA/RNA-binding protein TDP-43 (114, 115) plays a critical role in RNA processing, such as in alternative splicing, RNA stability, and transcriptional regulation in the CNS (116, 117). Hyperphosphorylated and ubiquitinated TDP-43 were accumulated in inclusion bodies in the brain and spinal cord of patients with frontotemporal lobar degeneration (FTLD) and amyotrophic lateral sclerosis (ALS) (118). Almost cases (90%) of ALS are sporadic, whereas familial ALS cases (10%) include the inheritance of mutations. The mutation (10%) in *TARDBP* that encodes TDP-43 and the remaining 90% are due to mutations in other genes (e.g., *C9ORF72, SOD1,* and *FUS*). From the unique gene *C9ORF72*, the transcribed RNA forms foci in neurons and glial cells and sequesters RNA-binding proteins, such as hnRNP43, in a mechanism that includes loss of C9ORF72 function (119). Assemblies of SOD1 (120) and FUS (114, 115) were also found in the inclusion bodies. Although SOD1, a metalloprotein that binds to copper and zinc ions, is not related to RNA binding, FUS is a known RNA-binding protein; thus, FUS is described in the next subsection.

TDP-43 consists of 414 amino acids and contains two RNA recognition motifs (also known as ribonucleoproteins: RRM1 at aa 101–176 and RRM2 at aa 191–262) (121, 122), and a C-terminal low-complexity domain (LCD: aa 274–414) (118, 123) (**Fig. 4a**). The LCD includes glutamine/asparagine rich and glycine rich domains and is unstructured and flexible with functions that differ from those in normal regions involved in structured regions. Molliex et al. reported that the phase separation by the LCD induced from TDP-43 promoted stress granule

assembly and TDP-43 aggregation (124). An accumulation of studies also suggest that the LCD is responsible for the propensity to form amyloid fibrils and stress granules (125). Notably, based on the moderate similarities in the sequence between the LCD and prion proteins from *Homo sapiens* and *Pan troglodytes*, TDP-43 is postulated to have prion-like properties (126); indeed, the LCD was found to be propagated intercellularly (cell to cell) as a trigger of disease progression (127). In particular, TDP-43 downregulated splicing of the exon 9 of cystic fibrosis transmembrane conductance regulator by binding to a UG repeat site in RRM1 based on electrophoretic mobility shift assay (EMSA) ($K_D$ = 27 nM) or isothermal titration calorimetry (ITC) ($K_D$ = 32 nM) (128, 129), and the fragment of TDP-43 showed stronger affinity ($K_D$ = 5.3 nM) to RNA including $(UG)_6$ using EMSA (130). NMR studies based on $^{1}H$-$^{15}N$ SOFAST-HMQC revealed the binding site in RRM1 loop3 and RRM2 pocket around V220 of TDP-43 (131). As observed in the case of RNA, TDP-43 associated with ssDNA containing $(TG)_{12}$ with potent binding affinity using ITC (132).

NMR studies by Conicella et al. showed that TDP-43 generated dimers through helix–helix contact (aa 321–343) in the LCD (133). Liquid-to-liquid phase separation (LLPS) is known to occur when two liquid phases coexist in nonmembrane organelles, and it drives the formation of biomolecular compartments, such as lipid droplets, for local biological reactions and signaling systems (134, 135). The experiments of these authors also revealed that the intermolecular helix–helix contact in the LCD induced the formation of liquid droplets of TDP-43, which generated amyloid fibrils upon their incubation. As validation, the nonpathological mutation (A321G) in the LCD disturbed the helical structure as well as liquid droplet formation, whereas an ALS-related mutation (G335D) in the LCD increased LLPS through stabilization of the helix structure (133). Fonda et al. conducted ssNMR analysis that showed that the liquid droplets from TDP-43 were transformed into β-strand-rich fibrils through stabilization of a region (aa 365–400) within the LCD (136). Cryo-EM analysis by Li et al. indicated that amyloid fibrils of TDP-43 in the LCD harbored a core architecture, including several β-strands that were linked by loop structures (33). These findings demonstrate that the LCD is indispensable to the aggregation of TDP-43.

Wang et al. used NMR to show that the interaction between N-terminal domains was involved in the dimerization of TDP-43 (137). Their study also showed that the S48E mutation inhibited the aggregation of TDP-43 and that liquid droplet formation was prevented by the failure to phosphorylate Ser48 (137). In TDP-43, RRM binding to RNA (e.g., long noncoding RNA) drove liquid-like granule formation within cells (138) together with the self-association of N-terminal domains as well as helix–helix contact within the LCD (137, 139). TDP-43 is also known as a shuttling protein that travels between the nucleus and cytoplasm to facilitate cellular functions. Indeed, it is normally localized in the nucleus (140), but it moves to the cytoplasm and aggregates to form insoluble inclusions in disease states (141). Under transient stress conditions, TDP-43 forms nuclear bodies for sheltering by binding long noncoding RNA in the nucleus. Subsequently, the transferred TDP-43 generates stress granules by bundling heterogeneous nuclear ribonucleoproteins (hnRNPs) and RNAs in the cytosol. Moreover, long-term physiological stress and senescence induce the formation of stress granules, leading

to maturation and transformation into inclusion bodies.

*FUS/TLS coaggregation with RNA*

The 526-mer RNA-binding protein FUS/TLS is a heterogeneous nuclear ribonucleoprotein P2 encoded by *FUS* (142, 143). In 2009, mutations in *FUS* were found to be causative in subtypes of ALS cases (144, 145). FUS play a pivotal role in RNA processing, splicing, and transport (146). It is mainly composed of a serine–tyrosine–glycine–glutamine rich LCD (aa 1–165) in the N-terminal region, three arginine–glycine-glycine (RGG) rich domains (aa 166–267, aa 372–422, and aa 453–501, respectively), a RRM (aa 285–371), a zinc finger motif (aa 422–453), and a highly conserved nuclear localization signal domain (aa 501–526) in the C-terminal region (147, 148). Using a bioinformatics approach, the presence of two prion-like domains was also discovered (aa 1–239 and 391–407) (149) (**Fig. 4a**). Tycko and colleagues first determined the structure of *in vitro* fibrils obtained from the LCD of FUS by ssNMR, showing that a segment of 61 residues formed the fibril core with a S-shaped fold and right-handed twist, which plays a role in LLPS (150). The following study using a different segment (91 residues) in LCD domain based on cryo-EM supports for this structural feature by ssNMR (151) (**Fig. 4b**). However, the *ex vivo* structure of FUS fibrils has not yet been determined.

FUS is normally localized in the nucleus, but it can shuttle between the nucleus and cytoplasm in a similar manner to TDP-43 (152). The FUS mutation in familial ALS hampers the signal for nuclear localization, leading to the accumulation of FUS in the cytoplasm and acquisition of gain-of-function toxicity via sequestration of RNA (153, 154). In one study, the accumulation of RNA-binding proteins in the pathogenesis of ALS was found to be seeded by granules of ribonucleoprotein (155). The granules composed of membraneless organelles were stabilized by LLPS, in which self-association was induced in the liquid droplets (156). These observations are in agreement with the immunoreactivity of FUS in the cytoplasmic inclusions of the brain of patients with ALS and FTLD. Moreover, these findings indicate that the mislocalization of FUS to the cytoplasm is a pathogenic trigger (157).

Lerga et al. found that RNA oligoribonucleotides bind to the FUS protein at the GGUG motif with a 250 nM affinity using EMSA test (158). Another study showed that the recruitment of FUS to DNA damage sites was modulated by the RGG domain (159). In addition to RGG domains, the zinc finder motif in FUS is related to its RNA binding (160, 161), and then the binding constant was determined to be 56 nM by Wang et al (162). Indeed, RGG domain in FUS extensively recognized G4RNA from r(UUAGGG)$_4$ ($K_D$ = 6.2 nM) (163). In the following two studies, RGG domain was also reported to bind G4RNA deduced from post-synaptic density protein 95 (PSD-95) using a steady-state fluorescence spectroscopy ($K_D$ = 28 nM) (164) and surface plasmon resonance (SPR) ($K_D$ = 3.2 nM) (165). On the other hand, the binding affinity of stem-loop RNA structure in hnRNPA2/B1 to RGG was weaker based on ITC analysis ($K_D$ = 9.2 μM) (166).

The C-terminal nuclear localization signal domain in FUS is known to bind to the nuclear input receptor to enable transportation of FUS from the cytoplasm to the nucleus. Most of the mutations found in familial ALS are concentrated in this C-terminal signaling domain.

Loss-of-function mutations for such signaling prevent FUS from being transported into the nucleus, resulting in its accumulation in the cytoplasm (167, 168). Evidence suggests the LCD is localized at the N-terminus of FUS and contributes to the phase transition of the protein, facilitating the self-assembly of the LCD (169). Taken together, these findings indicate that FUS is transported from the nucleus to the cytoplasm before phase separation forms granules, after which FUS reversibly aggregates. However, it is conceivable that self-assembly of the LCD in the disease state originates from mutations in familial ALS; in this case, FUS may irreversibly aggregate, possibly through the LLPS pathway.

*FMRpolyG coaggregation with RNA*

Fragile X-related tremor/ataxia syndrome (FXTAS) is a neurodegenerative disease that is characterized by CGG triplet repeat expansions in *FMR1* (170), a gene that encodes repeat-associated non-AUG (RAN) translation and produces the 153-mer RNA-binding protein FMRpolyG. FXTAS is characterized by neuronal death and ubiquitin-positive inclusions within neurons, which are composed of FMRpolyG aggregates (**Fig. 4a**). According to confocal microscopy observations, FMRpolyG forms dot-like aggregates in the mitochondria as well as in the nuclear inclusion for subcellular localization of FMRpolyG. Using neuronal cell culture models and a FXTAS transgenic mouse model, these assemblies were related to the disturbance of mRNA splicing and impairment of the respiratory chain (171). Kumar and colleagues screened a small molecule library (>250,000 molecules) and identified three candidates that prevent impaired mRNA splicing and bind CGG repeat RNAs [r(CGG × 20–60)] using a fluorescence binding test and isothermal calorimetry titration binding assay (172). These RNA binders also inhibited the aggregation of FMRpolyG and RAN translation, indicating that they are lead molecules for anti-FXTAS drug development.

G-quadruplex of RNA (G4RNA) plays an important role in mRNA translocation and translation in the axons, dendrites, and dendritic spine of neuronal networks (**Fig. 3b**). Transport of mRNA to the synapse contributes to synaptic plasticity and learning memory (173, 174). In particular, dendritic mRNA generates a complex with RNA-binding proteins in RNA granules. Bioinformatics analysis showed that the function of ~30% of known dendritic mRNA was related to G-quadruplex consensus in the 3′-untranslated region (175). Given that FMRpolyG recognizes G4RNA in target *FMR1* mRNA (176, 177), Brown et al. performed a microarray of immunoprecipitation of the mouse brain with FMRpolyG, identifying 432 mRNAs, ~70% of which included a G-quadruplex-forming sequence (178). Crystal structure analysis also showed that the RNA-binding motif in FMRpolyG possesses three K-homology domains (also known as KH domains), which were identified in human hnRNP, and one RGG box (179). Notably, based on X-ray crystallography analysis, RGG peptides could stabilize the G-tetrad unit for facilitation of the G-quadruplex (180). The recognition of FMRpolyG to the G-quadruplex probably disturbs protein translation and RNA localization in the pathology of FXTAS. FMRpolyG is also known to suppress the mRNA translation of other genes, including *APP* (181), *PP2Ac* (182), and *MAP1B* (183), in a similar manner to its effects on *FMR1*. These results provide a potential modulator of FMRpolyG for FXTAS therapy.

Shioda and colleagues described the direct interaction of CGG repeat-derived G4RNA with the polyglycine region of FMRpolyG and the generation of FMRpolyG–G4RNA coaggregates (184). Prior to liquid-to-solid transition, LLPS induced the coaggregation of FMRpolyG–G4RNA, which primarily interacted with exosomal proteins (e.g., PPIA, eEF1A1, PKM, and hnRNP A2B1) in the exosomes, resulting in prion-like propagation of cell to cell and neuronal dysfunction. The same group previously identified a G4-binding ligand, 5-aminolevulinic acid, which was metabolized to porphyrins protoporphyrin IX and hemin in cells (185, 186). Notably, oral administration of 5-aminolevulinic acid prevented not only RAN translation of FMRpolyG but also coaggregation of FMRpolyG with G4RNA, resulting in the rescue of impaired synaptic plasticity and learning behavior in a mouse model of FXTAS. Their findings suggest that 5-aminolevulinic acid is a promising drug lead for G4RNA prionoids (185, 186).

Generally, RNA loss of function and RAN translation (gain of function) are considered the two underling mechanisms of proteinopathies associated with repeat expansion disorders (187). These two mechanisms are not independent but synergistically induce the formation of LLPS-derived FMRpolyG coaggregates with CGG repeat-derived G4RNA. To date, FMRpolyG has not been structurally determined. Thus, further investigation to clarify the underlying mechanism responsible for FXTAS etiology will be required to facilitate the development of target-specific medicines with few adverse effects.

## Conclusions and future perspectives

It is hypothesized that cross-seeding between amyloids is dependent on conformations that lower the energy barrier for seeding. The mechanism of amyloid aggregate formation has yet to be clarified for most proteins, and a more profound understanding is required to facilitate antiamyloid drug design and discovery. The protein components involved in cross-seeding should be further investigated to clarify the role and underlying mechanism of cross-seeding aggregation. The inhibitors that dually target amyloidogenic proteins participating in the cross-seeding event can inhibit heterologous aggregation but also cause disassembly of the aggregates. Understanding the molecular mechanism underlying the interactions in cross-seeding will help researchers develop effective disease-modifying therapies for protein-misfolding diseases. Furthermore, by designing site-specific inhibitors, researchers could also develop new approaches to inhibit and disassemble both homologous and heterologous aggregates.

In 2022, using proteomics data of Aβ plaques from AD brains, Konstantoulea et al. found that heterotypic Aβ interacts with peptide fragments from human proteins to facilitate cross-seeding (188). These proteins shared local sequence homology with aggregation-prone regions within Aβ, and transient expression of three of these proteins (WD repeat-containing protein 81, chondroitin sulfate proteoglycan 5, and interferon regulatory factor 7) accelerated Aβ aggregation in a cellular reporter model. Although the amyloid core is believed to share a common interface with other amyloid species through a cross-β unit (189), the coaggregation hypothesis has been expanded to unrelated human proteins. Indeed, ectopic DNA, such as

bacterial extracellular DNA, has been shown to enhance aggregation of Aβ (190) and tau (191). However, β-sheet-triggered protein–nucleic acid interactions may also play a pivotal role in the stability, compartmentalization, and degradation-resistance of vital amyloid-related proteins (192). Although physiological and pathological differences may be subtle, the role of nucleic acids is supposedly dependent on the cellular environment for modulation of the balance between the two. Although an accumulation of evidence suggests that LLPS in the nucleus and cytoplasm is important in maintaining cellular homeostasis and advances have been made in the structural determination of amyloid assemblies, drugs targeting amyloid coaggregation have not yet advanced to clinical trials in the neurodegeneration disease field. To advance the development of anticoaggregation medicines for biomedical applications, several issues should be addressed as follows.

First, the conformational metastability and heterogeneity of coaggregates of amyloid oligomers with other amyloids or nucleic acids are major impediments for structural elucidation of complexes. This challenge can be addressed using cryo-EM for *ex vivo* amyloid fibrils, which could partially reflect the coaggregates with biomolecules, as demonstrated in the cases of Aβ40 (19, 25), Aβ42 (21, 28), tau (29), and TDP-43 (30). Although cryo-EM analyses combined with computational advancement have been applied to RNA structures (193) and structures of nucleoprotein–RNA complexes (194), there have been no such studies (to the best of our knowledge) on amyloid–RNA complexes.

Second, identification of the inhibitors harboring dual inhibition activities against different pairs of coaggregates is a promising approach that could increase both the speed and success of the process. Considering the existing common amyloid core in coaggregates, natural products with inhibitory activities against multiple (dual or triple) amyloid aggregates have been reported (as discussed above): benzylamino-2-hydroxyalkyl derivatives (195), a curcumin derivative (PE859) (196), notopterol (197), and epigallocatechin-3-gallate (198) against Aβ and tau aggregation; curcumin (199) against Aβ and αSyn aggregation; and a synthetic compound (MG-2119) (200) against tau and αSyn aggregation. Drug repositioning could also be successful in the case of entacapone and tolcapone, inhibitors of catechol-*O*-methyltransferase and anti-Parkinsonian drugs, which are also available as aggregation inhibitors against Aβ and αSyn aggregation. Development of nucleic acid binders will help obtain inhibitors of amyloid coaggregation with nucleic acids, as demonstrated by CGG repeat RNA binders in FXTAS therapeutics (172), and will also help clarify the molecular basis of amyloid recognition by nucleic acids. The increasing use of next-generation sequencing to sequence mRNA transcripts exhaustively suggests that additional data will be forthcoming.

Finally, the antagonistic function of nucleic acid medicine targeting nucleic acids, which can participate in the formation of amyloid coaggregates, is a promising lead in neurodegeneration therapeutics (9). Nucleic acid aptamers are potential candidates, especially in the antiamyloid field, and various aptamers against amyloidogenic proteins, including oligomeric assembly, have been developed. We expect that these aptamers will suppress the interactions of amyloid coaggregates and further aggregation by shifting equilibrium to the disaggregated state. There are several delivery systems to the CNS, such as exosomes and

nanoliposomes, and each system has advantages and limitations; future study should address the current shortcomings in the target specificity of aptamers, which could improve the delivery of aptamers into the CNS, as was demonstrated successfully for a DNA aptamer against αSyn (F5R1) using a model mouse with a synucleinopathy (201). Recent advances in both computational and experimental approaches suggest that antinucleic acid therapeutics will be realized in the near future. Overall, we have highlighted new mechanistic insights into amyloid coaggregation, which could pave the way for future studies on the underlying mechanisms and causes of neurodegenerative diseases.

**Competing interests**

The authors declare that they have no competing interests.

**Funding**

This study was supported in part by JSPS KAKENHI, grant number 20KK0126 to K.M, and grant number 19K07965 and 22K07514 to K.O.

**Author contributions**

K.M. and K.O. completed the literature search; planned, wrote, and revised the manuscript; and prepared the figures and tables.

**DATA AVAILABILITY STATEMENT**

This is not applicable for this review.

**References**

1. Iadanza, M. G., Jackson, M. P., Hewitt, E. W., Ranson, N. A., and Radford, S. E. (2018) A new era for understanding amyloid structures and disease. *Nat. Rev. Mol. Cell Biol.* **19**, 755-773
2. Hartl, F. U. (2017) Protein Misfolding Diseases. *Annu. Rev. Biochem.* **86**, 21-26
3. Ono, K. (2018) Alzheimer's disease as oligomeropathy. *Neurochem. Int.* **119**, 57-70
4. Chuang, E., Hori, A. M., Hesketh, C. D., and Shorter, J. (2018) Amyloid assembly and disassembly. *J. Cell Sci.* **131**, jcs189928
5. Otzen, D., and Riek, R. (2019) Functional amyloids. *Cold Spring Harb. Perspect. Biol.* **11**, a033860
6. Benilova, I., Karran, E., and De Strooper, B. (2012) The toxic Aβ oligomer and Alzheimer's disease: an emperor in need of clothes. *Nat. Neurosci.* **15**, 349-357
7. Bitan, G., Fradinger, E. A., Spring, S. M., and Teplow, D. B. (2005) Neurotoxic protein oligomers--what you see is not always what you get. *Amyloid* **12**, 88-95
8. Roychaudhuri, R., Yang, M., Hoshi, M. M., and Teplow, D. B. (2009) Amyloid β-protein assembly and Alzheimer disease. *J. Biol. Chem.* **284**, 4749-4753
9. Murakami, K., Izuo, N., and Bitan, G. (2022) Aptamers targeting amyloidogenic proteins and their emerging role in neurodegenerative diseases. *J. Biol. Chem.* **298**, 101478

10. Jarrett, J. T., and Lansbury, P. T., Jr. (1993) Seeding "one-dimensional crystallization" of amyloid: a pathogenic mechanism in Alzheimer's disease and scrapie? *Cell* **73**, 1055-1058
11. Esler, W. P., Stimson, E. R., Jennings, J. M., Vinters, H. V., Ghilardi, J. R., Lee, J. P., Mantyh, P. W., and Maggio, J. E. (2000) Alzheimer's disease amyloid propagation by a template-dependent dock-lock mechanism. *Biochemistry* **39**, 6288-6295
12. Zekry, D., Hauw, J. J., and Gold, G. (2002) Mixed dementia: epidemiology, diagnosis, and treatment. *J. Am. Geriatr. Soc.* **50**, 1431-1438
13. Irwin, D. J., Lee, V. M., and Trojanowski, J. Q. (2013) Parkinson's disease dementia: convergence of α-synuclein, tau and amyloid-β pathologies. *Nat. Rev. Neurosci.* **14**, 626-636
14. Moussaud, S., Jones, D. R., Moussaud-Lamodiere, E. L., Delenclos, M., Ross, O. A., and McLean, P. J. (2014) α-Synuclein and tau: teammates in neurodegeneration? *Mol. Neurodegener.* **9**, 43
15. Colom-Cadena, M., Gelpi, E., Charif, S., Belbin, O., Blesa, R., Marti, M. J., Clarimon, J., and Lleo, A. (2013) Confluence of α-synuclein, tau, and β-amyloid pathologies in dementia with Lewy bodies. *J. Neuropathol. Exp. Neurol.* **72**, 1203-1212
16. Spires-Jones, T. L., Attems, J., and Thal, D. R. (2017) Interactions of pathological proteins in neurodegenerative diseases. *Acta Neuropathol.* **134**, 187-205
17. Silva, J. L., and Cordeiro, Y. (2016) The "Jekyll and Hyde" actions of nucleic acids on the prion-like aggregation of proteins. *J. Biol. Chem.* **291**, 15482-15490
18. Conlon, E. G., and Manley, J. L. (2017) RNA-binding proteins in neurodegeneration: mechanisms in aggregate. *Genes Dev.* **31**, 1509-1528
19. Lu, J. X., Qiang, W., Yau, W. M., Schwieters, C. D., Meredith, S. C., and Tycko, R. (2013) Molecular structure of β-amyloid fibrils in Alzheimer's disease brain tissue. *Cell* **154**, 1257-1268
20. Paravastu, A. K., Leapman, R. D., Yau, W. M., and Tycko, R. (2008) Molecular structural basis for polymorphism in Alzheimer's β-amyloid fibrils. *Proc. Natl. Acad. Sci. U. S. A.* **105**, 18349-18354
21. Qiang, W., Yau, W. M., Lu, J. X., Collinge, J., and Tycko, R. (2017) Structural variation in amyloid-β fibrils from Alzheimer's disease clinical subtypes. *Nature* **541**, 217-221
22. Xiao, Y., Ma, B., McElheny, D., Parthasarathy, S., Long, F., Hoshi, M., Nussinov, R., and Ishii, Y. (2015) Aβ(1-42) fibril structure illuminates self-recognition and replication of amyloid in Alzheimer's disease. *Nat. Struc. Mol. Biol.* **22**, 499-505
23. Colvin, M. T., Silvers, R., Ni, Q. Z., Can, T. V., Sergeyev, I., Rosay, M., Donovan, K. J., Michael, B., Wall, J., Linse, S., and Griffin, R. G. (2016) Atomic resolution structure of monomorphic Aβ42 amyloid fibrils. *J. Am. Chem. Soc.* **138**, 9663-9674
24. Walti, M. A., Ravotti, F., Arai, H., Glabe, C. G., Wall, J. S., Bockmann, A., Guntert, P., Meier, B. H., and Riek, R. (2016) Atomic-resolution structure of a disease-relevant Aβ(1-42) amyloid fibril. *Proc. Natl. Acad. Sci. U. S. A.* **113**, E4976-4984

25. Kollmer, M., Close, W., Funk, L., Rasmussen, J., Bsoul, A., Schierhorn, A., Schmidt, M., Sigurdson, C. J., Jucker, M., and Fandrich, M. (2019) Cryo-EM structure and polymorphism of Aβ amyloid fibrils purified from Alzheimer's brain tissue. *Nat. Commun.* **10**, 4760
26. Meinhardt, J., Sachse, C., Hortschansky, P., Grigorieff, N., and Fandrich, M. (2009) Aβ(1-40) fibril polymorphism implies diverse interaction patterns in amyloid fibrils. *J. Mol. Biol.* **386**, 869-877
27. Schmidt, M., Sachse, C., Richter, W., Xu, C., Fandrich, M., and Grigorieff, N. (2009) Comparison of Alzheimer Aβ(1-40) and Aβ(1-42) amyloid fibrils reveals similar protofilament structures. *Proc. Natl. Acad. Sci. U. S. A.* **106**, 19813-19818
28. Yang, Y., Arseni, D., Zhang, W., Huang, M., Lovestam, S., Schweighauser, M., Kotecha, A., Murzin, A. G., Peak-Chew, S. Y., Macdonald, J., Lavenir, I., Garringer, H. J., Gelpi, E., Newell, K. L., Kovacs, G. G., Vidal, R., Ghetti, B., Ryskeldi-Falcon, B., Scheres, S. H. W., and Goedert, M. (2022) Cryo-EM structures of amyloid-β42 filaments from human brains. *Science* **375**, 167-172
29. Fitzpatrick, A. W. P., Falcon, B., He, S., Murzin, A. G., Murshudov, G., Garringer, H. J., Crowther, R. A., Ghetti, B., Goedert, M., and Scheres, S. H. W. (2017) Cryo-EM structures of tau filaments from Alzheimer's disease. *Nature* **547**, 185-190
30. Arseni, D., Hasegawa, M., Murzin, A. G., Kametani, F., Arai, M., Yoshida, M., and Ryskeldi-Falcon, B. (2022) Structure of pathological TDP-43 filaments from ALS with FTLD. *Nature* **601**, 139-143
31. Berriman, J., Serpell, L. C., Oberg, K. A., Fink, A. L., Goedert, M., and Crowther, R. A. (2003) Tau filaments from human brain and from in vitro assembly of recombinant protein show cross-β structure. *Proc. Natl. Acad. Sci. U. S. A.* **100**, 9034-9038
32. Cao, Q., Boyer, D. R., Sawaya, M. R., Ge, P., and Eisenberg, D. S. (2019) Cryo-EM structures of four polymorphic TDP-43 amyloid cores. *Nat. Struct. Mol. Biol.* **26**, 619-627
33. Li, Q., Babinchak, W. M., and Surewicz, W. K. (2021) Cryo-EM structure of amyloid fibrils formed by the entire low complexity domain of TDP-43. *Nat. Commun.* **12**, 1620
34. Goedert, M. (2015) NEURODEGENERATION. Alzheimer's and Parkinson's diseases: The prion concept in relation to assembled Aβ, tau, and α-synuclein. *Science* **349**, 1255555
35. Jucker, M., and Walker, L. C. (2013) Self-propagation of pathogenic protein aggregates in neurodegenerative diseases. *Nature* **501**, 45-51
36. Guo, J. P., Arai, T., Miklossy, J., and McGeer, P. L. (2006) Aβ and tau form soluble complexes that may promote self aggregation of both into the insoluble forms observed in Alzheimer's disease. *Proc. Natl. Acad. Sci. U. S. A.* **103**, 1953-1958
37. Gotz, J., Chen, F., van Dorpe, J., and Nitsch, R. M. (2001) Formation of neurofibrillary tangles in P301l tau transgenic mice induced by Aβ42 fibrils. *Science* **293**, 1491-1495
38. Lewis, J., Dickson, D. W., Lin, W. L., Chisholm, L., Corral, A., Jones, G., Yen, S. H., Sahara, N., Skipper, L., Yager, D., Eckman, C., Hardy, J., Hutton, M., and McGowan,

E. (2001) Enhanced neurofibrillary degeneration in transgenic mice expressing mutant tau and APP. *Science* **293**, 1487-1491

39. Hamilton, R. L. (2000) Lewy bodies in Alzheimer's disease: a neuropathological review of 145 cases using α-synuclein immunohistochemistry. *Brain Pathol.* **10**, 378-384

40. Uchikado, H., Lin, W. L., DeLucia, M. W., and Dickson, D. W. (2006) Alzheimer disease with amygdala Lewy bodies: a distinct form of α-synucleinopathy. *J. Neuropathol. Exp. Neurol.* **65**, 685-697

41. Toledo, J. B., Brettschneider, J., Grossman, M., Arnold, S. E., Hu, W. T., Xie, S. X., Lee, V. M., Shaw, L. M., and Trojanowski, J. Q. (2012) CSF biomarkers cutoffs: the importance of coincident neuropathological diseases. *Acta Neuropathol.* **124**, 23-35

42. Armstrong, R. A., Cairns, N. J., and Lantos, P. L. (1997) β-Amyloid (Aβ) deposition in the medial temporal lobe of patients with dementia with Lewy bodies. *Neurosci. Lett.* **227**, 193-196

43. Irwin, D. J., Grossman, M., Weintraub, D., Hurtig, H. I., Duda, J. E., Xie, S. X., Lee, E. B., Van Deerlin, V. M., Lopez, O. L., Kofler, J. K., Nelson, P. T., Jicha, G. A., Woltjer, R., Quinn, J. F., Kaye, J., Leverenz, J. B., Tsuang, D., Longfellow, K., Yearout, D., Kukull, W., Keene, C. D., Montine, T. J., Zabetian, C. P., and Trojanowski, J. Q. (2017) Neuropathological and genetic correlates of survival and dementia onset in synucleinopathies: a retrospective analysis. *Lancet Neurol.* **16**, 55-65

44. Masliah, E., Rockenstein, E., Veinbergs, I., Sagara, Y., Mallory, M., Hashimoto, M., and Mucke, L. (2001) β-Amyloid peptides enhance α-synuclein accumulation and neuronal deficits in a transgenic mouse model linking Alzheimer's disease and Parkinson's disease. *Proc. Natl. Acad. Sci. U. S. A.* **98**, 12245-12250

45. Mandal, P. K., Pettegrew, J. W., Masliah, E., Hamilton, R. L., and Mandal, R. (2006) Interaction between Aβ peptide and α synuclein: molecular mechanisms in overlapping pathology of Alzheimer's and Parkinson's in dementia with Lewy body disease. *Neurochem. Res.* **31**, 1153-1162

46. Ono, K. (2017) The oligomer hypothesis in α-synucleinopathy. *Neurochem. Res.* **42**, 3362-3371

47. Tsigelny, I. F., Crews, L., Desplats, P., Shaked, G. M., Sharikov, Y., Mizuno, H., Spencer, B., Rockenstein, E., Trejo, M., Platoshyn, O., Yuan, J. X., and Masliah, E. (2008) Mechanisms of hybrid oligomer formation in the pathogenesis of combined Alzheimer's and Parkinson's diseases. *PLoS One* **3**, e3135

48. Ono, K., Takahashi, R., Ikeda, T., and Yamada, M. (2012) Cross-seeding effects of amyloid β-protein and α-synuclein. *J. Neurochem.* **122**, 883-890

49. Guo, J. L., Covell, D. J., Daniels, J. P., Iba, M., Stieber, A., Zhang, B., Riddle, D. M., Kwong, L. K., Xu, Y., Trojanowski, J. Q., and Lee, V. M. (2013) Distinct α-synuclein strains differentially promote tau inclusions in neurons. *Cell* **154**, 103-117

50. Bassil, F., Brown, H. J., Pattabhiraman, S., Iwasyk, J. E., Maghames, C. M., Meymand, E. S., Cox, T. O., Riddle, D. M., Zhang, B., Trojanowski, J. Q., and Lee, V. M. (2020)

Amyloid-β (Aβ) Plaques promote seeding and spreading of α-synuclein and tau in a mouse model of Lewy body disorders with Aβ pathology. *Neuron* **105**, 260-275 e266

51. Zhao, J., Luo, Y., Jang, H., Yu, X., Wei, G., Nussinov, R., and Zheng, J. (2012) Probing ion channel activity of human islet amyloid polypeptide (amylin). *Biochim. Biophys. Acta* **1818**, 3121-3130
52. Subedi, S., Sasidharan, S., Nag, N., Saudagar, P., and Tripathi, T. (2022) Amyloid cross-seeding: mechanism, implication, and inhibition. *Molecules* **27**, 1776
53. Leibson, C. L., Rocca, W. A., Hanson, V. A., Cha, R., Kokmen, E., O'Brien, P. C., and Palumbo, P. J. (1997) Risk of dementia among persons with diabetes mellitus: a population-based cohort study. *Am. J. Epidemiol.* **145**, 301-308
54. Ott, A., Stolk, R. P., van Harskamp, F., Pols, H. A., Hofman, A., and Breteler, M. M. (1999) Diabetes mellitus and the risk of dementia: The Rotterdam study. *Neurology* **53**, 1937-1942
55. Bharadwaj, P., Solomon, T., Sahoo, B. R., Ignasiak, K., Gaskin, S., Rowles, J., Verdile, G., Howard, M. J., Bond, C. S., Ramamoorthy, A., Martins, R. N., and Newsholme, P. (2020) Amylin and β amyloid proteins interact to form amorphous heterocomplexes with enhanced toxicity in neuronal cells. *Sci. Rep.* **10**, 10356
56. Oskarsson, M. E., Paulsson, J. F., Schultz, S. W., Ingelsson, M., Westermark, P., and Westermark, G. T. (2015) In vivo seeding and cross-seeding of localized amyloidosis: a molecular link between type 2 diabetes and Alzheimer disease. *Am. J. Pathol.* **185**, 834-846
57. Martinez-Valbuena, I., Amat-Villegas, I., Valenti-Azcarate, R., Carmona-Abellan, M. D. M., Marcilla, I., Tunon, M. T., and Luquin, M. R. (2018) Interaction of amyloidogenic proteins in pancreatic β cells from subjects with synucleinopathies. *Acta Neuropathol.* **135**, 877-886
58. Mucibabic, M., Steneberg, P., Lidh, E., Straseviciene, J., Ziolkowska, A., Dahl, U., Lindahl, E., and Edlund, H. (2020) α-Synuclein promotes IAPP fibril formation in vitro and β-cell amyloid formation in vivo in mice. *Sci. Rep.* **10**, 20438
59. Tang, Y., Zhang, D., Liu, Y., Zhang, Y., Zhou, Y., Chang, Y., Zheng, B., Xu, A., and Zheng, J. (2022) A new strategy to reconcile amyloid cross-seeding and amyloid prevention in a binary system of α-synuclein fragmental peptide and hIAPP. *Protein Sci.* **31**, 485-497
60. Colon, W., and Kelly, J. W. (1992) Partial denaturation of transthyretin is sufficient for amyloid fibril formation in vitro. *Biochemistry* **31**, 8654-8660
61. Gharibyan, A. L., Wasana Jayaweera, S., Lehmann, M., Anan, I., and Olofsson, A. (2022) Endogenous human proteins interfering with amyloid formation. *Biomolecules* **12**, 446
62. Stein, T. D., Anders, N. J., DeCarli, C., Chan, S. L., Mattson, M. P., and Johnson, J. A. (2004) Neutralization of transthyretin reverses the neuroprotective effects of secreted amyloid precursor protein (APP) in APPSW mice resulting in tau phosphorylation and

loss of hippocampal neurons: support for the amyloid hypothesis. *J. Neurosci.* **24**, 7707-7717

63. Choi, S. H., Leight, S. N., Lee, V. M., Li, T., Wong, P. C., Johnson, J. A., Saraiva, M. J., and Sisodia, S. S. (2007) Accelerated Aβ deposition in APPswe/PS1deltaE9 mice with hemizygous deletions of TTR (transthyretin). *J. Neurosci.* **27**, 7006-7010
64. Nilsson, L., Pamren, A., Islam, T., Brannstrom, K., Golchin, S. A., Pettersson, N., Iakovleva, I., Sandblad, L., Gharibyan, A. L., and Olofsson, A. (2018) Transthyretin interferes with Aβ amyloid formation by redirecting oligomeric nuclei into non-amyloid aggregates. *J. Mol. Biol.* **430**, 2722-2733
65. Ghadami, S. A., Chia, S., Ruggeri, F. S., Meisl, G., Bemporad, F., Habchi, J., Cascella, R., Dobson, C. M., Vendruscolo, M., Knowles, T. P. J., and Chiti, F. (2020) Transthyretin inhibits primary and secondary nucleations of amyloid-β peptide aggregation and reduces the toxicity of its oligomers. *Biomacromolecules* **21**, 1112-1125
66. Wasana Jayaweera, S., Surano, S., Pettersson, N., Oskarsson, E., Lettius, L., Gharibyan, A. L., Anan, I., and Olofsson, A. (2021) Mechanisms of transthyretin inhibition of IAPP amyloid formation. *Biomolecules* **11**, 411
67. Mazzei, G., Ikegami, R., Abolhassani, N., Haruyama, N., Sakumi, K., Saito, T., Saido, T. C., and Nakabeppu, Y. (2021) A high-fat diet exacerbates the Alzheimer's disease pathology in the hippocampus of the *App*$^{NL-F/NL-F}$ knock-in mouse model. *Aging Cell* **20**, e13429
68. Hedlund, J., Johansson, J., and Persson, B. (2009) BRICHOS - a superfamily of multidomain proteins with diverse functions. *BMC Res. Notes* **2**, 180
69. Dolfe, L., Tambaro, S., Tigro, H., Del Campo, M., Hoozemans, J. J. M., Wiehager, B., Graff, C., Winblad, B., Ankarcrona, M., Kaldmae, M., Teunissen, C. E., Ronnback, A., Johansson, J., and Presto, J. (2018) The Bri2 and Bri3 BRICHOS domains interact differently with Aβ42 and Alzheimer amyloid plaques. *J. Alzheimers Dis. Rep.* **2**, 27-39
70. Hermansson, E., Schultz, S., Crowther, D., Linse, S., Winblad, B., Westermark, G., Johansson, J., and Presto, J. (2014) The chaperone domain BRICHOS prevents CNS toxicity of amyloid-β peptide in Drosophila melanogaster. *Dis. Model. Mech.* **7**, 659-665
71. Poska, H., Haslbeck, M., Kurudenkandy, F. R., Hermansson, E., Chen, G., Kostallas, G., Abelein, A., Biverstal, H., Crux, S., Fisahn, A., Presto, J., and Johansson, J. (2016) Dementia-related Bri2 BRICHOS is a versatile molecular chaperone that efficiently inhibits Aβ42 toxicity in Drosophila. *Biochem. J.* **473**, 3683-3704
72. Cohen, S. I. A., Arosio, P., Presto, J., Kurudenkandy, F. R., Biverstal, H., Dolfe, L., Dunning, C., Yang, X., Frohm, B., Vendruscolo, M., Johansson, J., Dobson, C. M., Fisahn, A., Knowles, T. P. J., and Linse, S. (2015) A molecular chaperone breaks the catalytic cycle that generates toxic Aβ oligomers. *Nat. Struct. Mol. Biol.* **22**, 207-213
73. Chen, G., Abelein, A., Nilsson, H. E., Leppert, A., Andrade-Talavera, Y., Tambaro, S., Hemmingsson, L., Roshan, F., Landreh, M., Biverstal, H., Koeck, P. J. B., Presto, J.,

Hebert, H., Fisahn, A., and Johansson, J. (2017) Bri2 BRICHOS client specificity and chaperone activity are governed by assembly state. *Nat. Commun.* **8**, 2081

74. Poska, H., Leppert, A., Tigro, H., Zhong, X., Kaldmae, M., Nilsson, H. E., Hebert, H., Chen, G., and Johansson, J. (2020) Recombinant Bri3 BRICHOS domain is a molecular chaperone with effect against amyloid formation and non-fibrillar protein aggregation. *Sci. Rep.* **10**, 9817
75. Oskarsson, M. E., Hermansson, E., Wang, Y., Welsh, N., Presto, J., Johansson, J., and Westermark, G. T. (2018) BRICHOS domain of Bri2 inhibits islet amyloid polypeptide (IAPP) fibril formation and toxicity in human β cells. *Proc. Natl. Acad. Sci. U. S. A.* **115**, E2752-E2761
76. Ginsberg, S. D., Galvin, J. E., Chiu, T. S., Lee, V. M., Masliah, E., and Trojanowski, J. Q. (1998) RNA sequestration to pathological lesions of neurodegenerative diseases. *Acta Neuropathol.* **96**, 487-494
77. Ginsberg, S. D., Crino, P. B., Hemby, S. E., Weingarten, J. A., Lee, V. M., Eberwine, J. H., and Trojanowski, J. Q. (1999) Predominance of neuronal mRNAs in individual Alzheimer's disease senile plaques. *Ann. Neurol.* **45**, 174-181
78. Marcinkiewicz, M. (2002) βAPP and furin mRNA concentrates in immature senile plaques in the brain of Alzheimer patients. *J. Neuropathol. Exp. Neurol.* **61**, 815-829
79. Silva, J. L., Lima, L. M., Foguel, D., and Cordeiro, Y. (2008) Intriguing nucleic-acid-binding features of mammalian prion protein. *Trends Biochem. Sci.* **33**, 132-140
80. Silva, J. L., Gomes, M. P., Vieira, T. C., and Cordeiro, Y. (2010) PrP interactions with nucleic acids and glycosaminoglycans in function and disease. *Front. Biosci. (Landmark Ed)* **15**, 132-150
81. Deleault, N. R., Piro, J. R., Walsh, D. J., Wang, F., Ma, J., Geoghegan, J. C., and Supattapone, S. (2012) Isolation of phosphatidylethanolamine as a solitary cofactor for prion formation in the absence of nucleic acids. *Proc. Natl. Acad. Sci. U. S. A.* **109**, 8546-8551
82. Calamai, M., Taddei, N., Stefani, M., Ramponi, G., and Chiti, F. (2003) Relative influence of hydrophobicity and net charge in the aggregation of two homologous proteins. *Biochemistry* **42**, 15078-15083
83. Shu, Y., Pi, F., Sharma, A., Rajabi, M., Haque, F., Shu, D., Leggas, M., Evers, B. M., and Guo, P. (2014) Stable RNA nanoparticles as potential new generation drugs for cancer therapy. *Adv. Drug Deliv. Rev*. **66**, 74-89
84. Prusiner, S. B., Scott, M. R., DeArmond, S. J., and Cohen, F. E. (1998) Prion protein biology. *Cell* **93**, 337-348
85. Collinge, J. (2001) Prion diseases of humans and animals: their causes and molecular basis. *Annu. Rev. Neurosci.* **24**, 519-550
86. Aguzzi, A., and Polymenidou, M. (2004) Mammalian prion biology: one century of evolving concepts. *Cell* **116**, 313-327

87. Louka, A., Zacco, E., Temussi, P. A., Tartaglia, G. G., and Pastore, A. (2020) RNA as the stone guest of protein aggregation. *Nucleic Acids Res.* **48**, 11880-11889

88. McLennan, N. F., Brennan, P. M., McNeill, A., Davies, I., Fotheringham, A., Rennison, K. A., Ritchie, D., Brannan, F., Head, M. W., Ironside, J. W., Williams, A., and Bell, J. E. (2004) Prion protein accumulation and neuroprotection in hypoxic brain damage. *Am. J. Pathol.* **165**, 227-235

89. Mitteregger, G., Vosko, M., Krebs, B., Xiang, W., Kohlmannsperger, V., Nolting, S., Hamann, G. F., and Kretzschmar, H. A. (2007) The role of the octarepeat region in neuroprotective function of the cellular prion protein. *Brain Pathol.* **17**, 174-183

90. Sengupta, I., and Udgaonkar, J. B. (2018) Structural mechanisms of oligomer and amyloid fibril formation by the prion protein. *Chem. Commun. (Camb.)* **54**, 6230-6242

91. Nandi, P. K. (1997) Interaction of prion peptide HuPrP106-126 with nucleic acid. *Arch. Virol.* **142**, 2537-2545

92. Nandi, P. K. (1998) Polymerization of human prion peptide HuPrP 106-126 to amyloid in nucleic acid solution. *Arch. Virol.* **143**, 1251-1263

93. Nandi, P. K., and Leclerc, E. (1999) Polymerization of murine recombinant prion protein in nucleic acid solution. *Arch. Virol.* **144**, 1751-1763

94. Cordeiro, Y., Machado, F., Juliano, L., Juliano, M. A., Brentani, R. R., Foguel, D., and Silva, J. L. (2001) DNA converts cellular prion protein into the β-sheet conformation and inhibits prion peptide aggregation. *J. Biol. Chem.* **276**, 49400-49409

95. Macedo, B., Millen, T. A., Braga, C. A., Gomes, M. P., Ferreira, P. S., Kraineva, J., Winter, R., Silva, J. L., and Cordeiro, Y. (2012) Nonspecific prion protein-nucleic acid interactions lead to different aggregates and cytotoxic species. *Biochemistry* **51**, 5402-5413

96. Cavaliere, P., Pagano, B., Granata, V., Prigent, S., Rezaei, H., Giancola, C., and Zagari, A. (2013) Cross-talk between prion protein and quadruplex-forming nucleic acids: a dynamic complex formation. *Nucleic Acids Res.* **41**, 327-339

97. Davis, J. T. (2004) G-quartets 40 years later: from 5'-GMP to molecular biology and supramolecular chemistry. *Angew. Chem. Int. Ed. Engl.* **43**, 668-698

98. Lima, L. M., Cordeiro, Y., Tinoco, L. W., Marques, A. F., Oliveira, C. L., Sampath, S., Kodali, R., Choi, G., Foguel, D., Torriani, I., Caughey, B., and Silva, J. L. (2006) Structural insights into the interaction between prion protein and nucleic acid. *Biochemistry* **45**, 9180-9187

99. Gomes, M. P., Millen, T. A., Ferreira, P. S., e Silva, N. L., Vieira, T. C., Almeida, M. S., Silva, J. L., and Cordeiro, Y. (2008) Prion protein complexed to N2a cellular RNAs through its N-terminal domain forms aggregates and is toxic to murine neuroblastoma cells. *J. Biol. Chem.* **283**, 19616-19625

100. Deleault, N. R., Lucassen, R. W., and Supattapone, S. (2003) RNA molecules stimulate prion protein conversion. *Nature* **425**, 717-720

101. Saborio, G. P., Permanne, B., and Soto, C. (2001) Sensitive detection of pathological prion protein by cyclic amplification of protein misfolding. *Nature* **411**, 810-813

102. Olsthoorn, R. C. (2014) G-quadruplexes within prion mRNA: the missing link in prion disease? *Nucleic Acids Res.* **42**, 9327-9333

103. Staple, D. W., and Butcher, S. E. (2005) Pseudoknots: RNA structures with diverse functions. *PLoS Biol.* **3**, e213

104. Bera, A., and Biring, S. (2018) A quantitative characterization of interaction between prion protein with nucleic acids. *Biochem. Biophys. Rep.* **14**, 114-124

105. Strom, A., Wang, G. S., Picketts, D. J., Reimer, R., Stuke, A. W., and Scott, F. W. (2011) Cellular prion protein localizes to the nucleus of endocrine and neuronal cells and interacts with structural chromatin components. *Eur. J. Cell Biol.* **90**, 414-419

106. Mange, A., Crozet, C., Lehmann, S., and Beranger, F. (2004) Scrapie-like prion protein is translocated to the nuclei of infected cells independently of proteasome inhibition and interacts with chromatin. *J. Cell Sci.* **117**, 2411-2416

107. Marijanovic, Z., Caputo, A., Campana, V., and Zurzolo, C. (2009) Identification of an intracellular site of prion conversion. *PLoS Pathog.* **5**, e1000426

108. Beaudoin, S., Vanderperre, B., Grenier, C., Tremblay, I., Leduc, F., and Roucou, X. (2009) A large ribonucleoprotein particle induced by cytoplasmic PrP shares striking similarities with the chromatoid body, an RNA granule predicted to function in posttranscriptional gene regulation. *Biochim. Biophys. Acta* **1793**, 335-345

109. Baron, G. S., Magalhaes, A. C., Prado, M. A., and Caughey, B. (2006) Mouse-adapted scrapie infection of SN56 cells: greater efficiency with microsome-associated versus purified PrP-res. *J. Virol.* **80**, 2106-2117

110. Rouvinski, A., Karniely, S., Kounin, M., Moussa, S., Goldberg, M. D., Warburg, G., Lyakhovetsky, R., Papy-Garcia, D., Kutzsche, J., Korth, C., Carlson, G. A., Godsave, S. F., Peters, P. J., Luhr, K., Kristensson, K., and Taraboulos, A. (2014) Live imaging of prions reveals nascent PrPSc in cell-surface, raft-associated amyloid strings and webs. *J. Cell Biol.* **204**, 423-441

111. Brown, D. R., Clive, C., and Haswell, S. J. (2001) Antioxidant activity related to copper binding of native prion protein. *J. Neurochem.* **76**, 69-76

112. Brown, D. R. (2003) Prion protein expression modulates neuronal copper content. *J. Neurochem.* **87**, 377-385

113. Liu, M., Yu, S., Yang, J., Yin, X., and Zhao, D. (2007) RNA and CuCl2 induced conformational changes of the recombinant ovine prion protein. *Mol. Cell. Biochem.* **294**, 197-203

114. Neumann, M., Sampathu, D. M., Kwong, L. K., Truax, A. C., Micsenyi, M. C., Chou, T. T., Bruce, J., Schuck, T., Grossman, M., Clark, C. M., McCluskey, L. F., Miller, B. L., Masliah, E., Mackenzie, I. R., Feldman, H., Feiden, W., Kretzschmar, H. A., Trojanowski, J. Q., and Lee, V. M. (2006) Ubiquitinated TDP-43 in frontotemporal lobar degeneration and amyotrophic lateral sclerosis. *Science* **314**, 130-133

115. Arai, T., Hasegawa, M., Akiyama, H., Ikeda, K., Nonaka, T., Mori, H., Mann, D., Tsuchiya, K., Yoshida, M., Hashizume, Y., and Oda, T. (2006) TDP-43 is a component

of ubiquitin-positive tau-negative inclusions in frontotemporal lobar degeneration and amyotrophic lateral sclerosis. *Biochem. Biophys. Res. Commun.* **351**, 602-611

116. Sephton, C. F., Cenik, B., Cenik, B. K., Herz, J., and Yu, G. (2012) TDP-43 in central nervous system development and function: clues to TDP-43-associated neurodegeneration. *Biol. Chem.* **393**, 589-594

117. Donde, A., Sun, M., Ling, J. P., Braunstein, K. E., Pang, B., Wen, X., Cheng, X., Chen, L., and Wong, P. C. (2019) Splicing repression is a major function of TDP-43 in motor neurons. *Acta Neuropathol.* **138**, 813-826

118. Prasad, A., Bharathi, V., Sivalingam, V., Girdhar, A., and Patel, B. K. (2019) Molecular mechanisms of TDP-43 misfolding and pathology in amyotrophic lateral sclerosis. *Front. Mol. Neurosci.* **12**, 25

119. Mori, K., Lammich, S., Mackenzie, I. R., Forne, I., Zilow, S., Kretzschmar, H., Edbauer, D., Janssens, J., Kleinberger, G., Cruts, M., Herms, J., Neumann, M., Van Broeckhoven, C., Arzberger, T., and Haass, C. (2013) hnRNP A3 binds to GGGGCC repeats and is a constituent of p62-positive/TDP43-negative inclusions in the hippocampus of patients with C9orf72 mutations. *Acta Neuropathol.* **125**, 413-423

120. Bruijn, L. I., Becher, M. W., Lee, M. K., Anderson, K. L., Jenkins, N. A., Copeland, N. G., Sisodia, S. S., Rothstein, J. D., Borchelt, D. R., Price, D. L., and Cleveland, D. W. (1997) ALS-linked SOD1 mutant G85R mediates damage to astrocytes and promotes rapidly progressive disease with SOD1-containing inclusions. *Neuron* **18**, 327-338

121. Lukavsky, P. J., Daujotyte, D., Tollervey, J. R., Ule, J., Stuani, C., Buratti, E., Baralle, F. E., Damberger, F. F., and Allain, F. H. (2013) Molecular basis of UG-rich RNA recognition by the human splicing factor TDP-43. *Nat. Struct. Mol. Biol.* **20**, 1443-1449

122. Kuo, P. H., Chiang, C. H., Wang, Y. T., Doudeva, L. G., and Yuan, H. S. (2014) The crystal structure of TDP-43 RRM1-DNA complex reveals the specific recognition for UG- and TG-rich nucleic acids. *Nucleic Acids Res.* **42**, 4712-4722

123. Kabashi, E., Valdmanis, P. N., Dion, P., Spiegelman, D., McConkey, B. J., Vande Velde, C., Bouchard, J. P., Lacomblez, L., Pochigaeva, K., Salachas, F., Pradat, P. F., Camu, W., Meininger, V., Dupre, N., and Rouleau, G. A. (2008) TARDBP mutations in individuals with sporadic and familial amyotrophic lateral sclerosis. *Nat. Genet.* **40**, 572-574

124. Molliex, A., Temirov, J., Lee, J., Coughlin, M., Kanagaraj, A. P., Kim, H. J., Mittag, T., and Taylor, J. P. (2015) Phase separation by low complexity domains promotes stress granule assembly and drives pathological fibrillization. *Cell* **163**, 123-133

125. Berning, B. A., and Walker, A. K. (2019) The pathobiology of TDP-43 C-terminal fragments in ALS and FTLD. *Front. Neurosci.* **13**, 335

126. Nonaka, T., and Hasegawa, M. (2020) Prion-like properties of assembled TDP-43. *Curr. Opin. Neurobiol.* **61**, 23-28

127. Feiler, M. S., Strobel, B., Freischmidt, A., Helferich, A. M., Kappel, J., Brewer, B. M., Li, D., Thal, D. R., Walther, P., Ludolph, A. C., Danzer, K. M., and Weishaupt, J. H.

(2015) TDP-43 is intercellularly transmitted across axon terminals. *J. Cell Biol.* **211**, 897-911

128. Ayala, Y. M., Pantano, S., D'Ambrogio, A., Buratti, E., Brindisi, A., Marchetti, C., Romano, M., and Baralle, F. E. (2005) Human, Drosophila, and C.elegans TDP43: nucleic acid binding properties and splicing regulatory function. *J. Mol. Biol.* **348**, 575-588

129. Brown, A. L., Wilkins, O. G., Keuss, M. J., Hill, S. E., Zanovello, M., Lee, W. C., Bampton, A., Lee, F. C. Y., Masino, L., Qi, Y. A., Bryce-Smith, S., Gatt, A., Hallegger, M., Fagegaltier, D., Phatnani, H., Consortium, N. A., Newcombe, J., Gustavsson, E. K., Seddighi, S., Reyes, J. F., Coon, S. L., Ramos, D., Schiavo, G., Fisher, E. M. C., Raj, T., Secrier, M., Lashley, T., Ule, J., Buratti, E., Humphrey, J., Ward, M. E., and Fratta, P. (2022) TDP-43 loss and ALS-risk SNPs drive mis-splicing and depletion of UNC13A. *Nature* **603**, 131-137

130. Bhardwaj, A., Myers, M. P., Buratti, E., and Baralle, F. E. (2013) Characterizing TDP-43 interaction with its RNA targets. *Nucleic Acids Res.* **41**, 5062-5074

131. Rengifo-Gonzalez, J. C., El Hage, K., Clement, M. J., Steiner, E., Joshi, V., Craveur, P., Durand, D., Pastre, D., and Bouhss, A. (2021) The cooperative binding of TDP-43 to GU-rich RNA repeats antagonizes TDP-43 aggregation. *Elife* **10**, e67605

132. Kitamura, A., Shibasaki, A., Takeda, K., Suno, R., and Kinjo, M. (2018) Analysis of the substrate recognition state of TDP-43 to single-stranded DNA using fluorescence correlation spectroscopy. *Biochem. Biophys. Rep.* **14**, 58-63

133. Conicella, A. E., Dignon, G. L., Zerze, G. H., Schmidt, H. B., D'Ordine, A. M., Kim, Y. C., Rohatgi, R., Ayala, Y. M., Mittal, J., and Fawzi, N. L. (2020) TDP-43 α-helical structure tunes liquid-liquid phase separation and function. *Proc. Natl. Acad. Sci. U. S. A.* **117**, 5883-5894

134. Hyman, A. A., Weber, C. A., and Julicher, F. (2014) Liquid-liquid phase separation in biology. *Annu. Rev. Cell Dev. Biol.* **30**, 39-58

135. Boeynaems, S., Alberti, S., Fawzi, N. L., Mittag, T., Polymenidou, M., Rousseau, F., Schymkowitz, J., Shorter, J., Wolozin, B., Van Den Bosch, L., Tompa, P., and Fuxreiter, M. (2018) Protein phase separation: A new phase in cell biology. *Trends Cell Biol.* **28**, 420-435

136. Fonda, B. D., Jami, K. M., Boulos, N. R., and Murray, D. T. (2021) Identification of the rigid core for aged liquid droplets of an RNA-binding protein low complexity domain. *J. Am. Chem. Soc.* **143**, 6657-6668

137. Wang, A., Conicella, A. E., Schmidt, H. B., Martin, E. W., Rhoads, S. N., Reeb, A. N., Nourse, A., Ramirez Montero, D., Ryan, V. H., Rohatgi, R., Shewmaker, F., Naik, M. T., Mittag, T., Ayala, Y. M., and Fawzi, N. L. (2018) A single N-terminal phosphomimic disrupts TDP-43 polymerization, phase separation, and RNA splicing. *EMBO J.* **37**, e97452

138. Khalfallah, Y., Kuta, R., Grasmuck, C., Prat, A., Durham, H. D., and Vande Velde, C. (2018) TDP-43 regulation of stress granule dynamics in neurodegenerative disease-relevant cell types. *Sci. Rep.* **8**, 7551

139. Chang, C. K., Wu, T. H., Wu, C. Y., Chiang, M. H., Toh, E. K., Hsu, Y. C., Lin, K. F., Liao, Y. H., Huang, T. H., and Huang, J. J. (2012) The N-terminus of TDP-43 promotes its oligomerization and enhances DNA binding affinity. *Biochem. Biophys. Res. Commun.* **425**, 219-224

140. Ayala, Y. M., Zago, P., D'Ambrogio, A., Xu, Y. F., Petrucelli, L., Buratti, E., and Baralle, F. E. (2008) Structural determinants of the cellular localization and shuttling of TDP-43. *J. Cell Sci.* **121**, 3778-3785

141. Winton, M. J., Igaz, L. M., Wong, M. M., Kwong, L. K., Trojanowski, J. Q., and Lee, V. M. (2008) Disturbance of nuclear and cytoplasmic TAR DNA-binding protein (TDP-43) induces disease-like redistribution, sequestration, and aggregate formation. *J. Biol. Chem.* **283**, 13302-13309

142. Crozat, A., Aman, P., Mandahl, N., and Ron, D. (1993) Fusion of CHOP to a novel RNA-binding protein in human myxoid liposarcoma. *Nature* **363**, 640-644

143. Calvio, C., Neubauer, G., Mann, M., and Lamond, A. I. (1995) Identification of hnRNP P2 as TLS/FUS using electrospray mass spectrometry. *RNA* **1**, 724-733

144. Kwiatkowski, T. J., Jr., Bosco, D. A., Leclerc, A. L., Tamrazian, E., Vanderburg, C. R., Russ, C., Davis, A., Gilchrist, J., Kasarskis, E. J., Munsat, T., Valdmanis, P., Rouleau, G. A., Hosler, B. A., Cortelli, P., de Jong, P. J., Yoshinaga, Y., Haines, J. L., Pericak-Vance, M. A., Yan, J., Ticozzi, N., Siddique, T., McKenna-Yasek, D., Sapp, P. C., Horvitz, H. R., Landers, J. E., and Brown, R. H., Jr. (2009) Mutations in the FUS/TLS gene on chromosome 16 cause familial amyotrophic lateral sclerosis. *Science* **323**, 1205-1208

145. Vance, C., Rogelj, B., Hortobagyi, T., De Vos, K. J., Nishimura, A. L., Sreedharan, J., Hu, X., Smith, B., Ruddy, D., Wright, P., Ganesalingam, J., Williams, K. L., Tripathi, V., Al-Saraj, S., Al-Chalabi, A., Leigh, P. N., Blair, I. P., Nicholson, G., de Belleroche, J., Gallo, J. M., Miller, C. C., and Shaw, C. E. (2009) Mutations in FUS, an RNA processing protein, cause familial amyotrophic lateral sclerosis type 6. *Science* **323**, 1208-1211

146. Sama, R. R., Ward, C. L., and Bosco, D. A. (2014) Functions of FUS/TLS from DNA repair to stress response: implications for ALS. *ASN Neuro.* **6**, 1759091414544472

147. Deng, H., Gao, K., and Jankovic, J. (2014) The role of FUS gene variants in neurodegenerative diseases. *Nat. Rev. Neurol.* **10**, 337-348

148. Nolan, M., Talbot, K., and Ansorge, O. (2016) Pathogenesis of FUS-associated ALS and FTD: insights from rodent models. *Acta Neuropathol. Commun.* **4**, 99

149. Sun, Z., Diaz, Z., Fang, X., Hart, M. P., Chesi, A., Shorter, J., and Gitler, A. D. (2011) Molecular determinants and genetic modifiers of aggregation and toxicity for the ALS disease protein FUS/TLS. *PLoS Biol.* **9**, e1000614

150. Murray, D. T., Kato, M., Lin, Y., Thurber, K. R., Hung, I., McKnight, S. L., and Tycko, R. (2017) Structure of FUS protein fibrils and its relevance to self-assembly and phase separation of low-complexity domains. *Cell* **171**, 615-627 e616

151. Sun, Y., Zhang, S., Hu, J., Tao, Y., Xia, W., Gu, J., Li, Y., Cao, Q., Li, D., and Liu, C. (2022) Molecular structure of an amyloid fibril formed by FUS low-complexity domain. *iScience* **25**, 103701

152. Andersson, M. K., Stahlberg, A., Arvidsson, Y., Olofsson, A., Semb, H., Stenman, G., Nilsson, O., and Aman, P. (2008) The multifunctional FUS, EWS and TAF15 proto-oncoproteins show cell type-specific expression patterns and involvement in cell spreading and stress response. *BMC Cell Biol.* **9**, 37

153. Scekic-Zahirovic, J., Sendscheid, O., El Oussini, H., Jambeau, M., Sun, Y., Mersmann, S., Wagner, M., Dieterle, S., Sinniger, J., Dirrig-Grosch, S., Drenner, K., Birling, M. C., Qiu, J., Zhou, Y., Li, H., Fu, X. D., Rouaux, C., Shelkovnikova, T., Witting, A., Ludolph, A. C., Kiefer, F., Storkebaum, E., Lagier-Tourenne, C., and Dupuis, L. (2016) Toxic gain of function from mutant FUS protein is crucial to trigger cell autonomous motor neuron loss. *EMBO J.* **35**, 1077-1097

154. Sharma, A., Lyashchenko, A. K., Lu, L., Nasrabady, S. E., Elmaleh, M., Mendelsohn, M., Nemes, A., Tapia, J. C., Mentis, G. Z., and Shneider, N. A. (2016) ALS-associated mutant FUS induces selective motor neuron degeneration through toxic gain of function. *Nat. Commun.* **7**, 10465

155. Li, Y. R., King, O. D., Shorter, J., and Gitler, A. D. (2013) Stress granules as crucibles of ALS pathogenesis. *J. Cell Biol.* **201**, 361-372

156. Courchaine, E. M., Lu, A., and Neugebauer, K. M. (2016) Droplet organelles? *EMBO J.* **35**, 1603-1612

157. Bosco, D. A., Lemay, N., Ko, H. K., Zhou, H., Burke, C., Kwiatkowski, T. J., Jr., Sapp, P., McKenna-Yasek, D., Brown, R. H., Jr., and Hayward, L. J. (2010) Mutant FUS proteins that cause amyotrophic lateral sclerosis incorporate into stress granules. *Hum. Mol. Genet.* **19**, 4160-4175

158. Lerga, A., Hallier, M., Delva, L., Orvain, C., Gallais, I., Marie, J., and Moreau-Gachelin, F. (2001) Identification of an RNA binding specificity for the potential splicing factor TLS. *J. Biol. Chem.* **276**, 6807-6816

159. Mastrocola, A. S., Kim, S. H., Trinh, A. T., Rodenkirch, L. A., and Tibbetts, R. S. (2013) The RNA-binding protein fused in sarcoma (FUS) functions downstream of poly(ADP-ribose) polymerase (PARP) in response to DNA damage. *J. Biol. Chem.* **288**, 24731-24741

160. Zinszner, H., Sok, J., Immanuel, D., Yin, Y., and Ron, D. (1997) TLS (FUS) binds RNA in vivo and engages in nucleo-cytoplasmic shuttling. *J. Cell Sci.* **110 (Pt 15)**, 1741-1750

161. Iko, Y., Kodama, T. S., Kasai, N., Oyama, T., Morita, E. H., Muto, T., Okumura, M., Fujii, R., Takumi, T., Tate, S., and Morikawa, K. (2004) Domain architectures and characterization of an RNA-binding protein, TLS. *J. Biol. Chem.* **279**, 44834-44840

1182 162. Wang, X., Schwartz, J. C., and Cech, T. R. (2015) Nucleic acid-binding specificity of
1183 human FUS protein. *Nucleic Acids Res.* **43**, 7535-7543
1184 163. Yagi, R., Miyazaki, T., and Oyoshi, T. (2018) G-quadruplex binding ability of
1185 TLS/FUS depends on the β-spiral structure of the RGG domain. *Nucleic Acids Res.* **46**,
1186 5894-5901
1187 164. Imperatore, J. A., McAninch, D. S., Valdez-Sinon, A. N., Bassell, G. J., and
1188 Mihailescu, M. R. (2020) FUS recognizes G quadruplex structures within neuronal
1189 mRNAs. *Front Mol Biosci* **7**, 6
1190 165. Ishiguro, A., Lu, J., Ozawa, D., Nagai, Y., and Ishihama, A. (2021) ALS-linked FUS
1191 mutations dysregulate G-quadruplex-dependent liquid-liquid phase separation and
1192 liquid-to-solid transition. *J. Biol. Chem.* **297**, 101284
1193 166. Loughlin, F. E., Lukavsky, P. J., Kazeeva, T., Reber, S., Hock, E. M., Colombo, M.,
1194 Von Schroetter, C., Pauli, P., Clery, A., Muhlemann, O., Polymenidou, M., Ruepp, M.
1195 D., and Allain, F. H. (2019) The solution structure of FUS bound to RNA reveals a
1196 bipartite mode of RNA recognition with both sequence and shape specificity. *Mol. Cell*
1197 **73**, 490-504 e6
1198 167. Lee, B. J., Cansizoglu, A. E., Suel, K. E., Louis, T. H., Zhang, Z., and Chook, Y. M.
1199 (2006) Rules for nuclear localization sequence recognition by karyopherin β2. *Cell* **126**,
1200 543-558
1201 168. Zhang, Z. C., and Chook, Y. M. (2012) Structural and energetic basis of ALS-causing
1202 mutations in the atypical proline-tyrosine nuclear localization signal of the Fused in
1203 Sarcoma protein (FUS). *Proc. Natl. Acad. Sci. U. S. A.* **109**, 12017-12021
1204 169. Li, P., Banjade, S., Cheng, H. C., Kim, S., Chen, B., Guo, L., Llaguno, M.,
1205 Hollingsworth, J. V., King, D. S., Banani, S. F., Russo, P. S., Jiang, Q. X., Nixon, B. T.,
1206 and Rosen, M. K. (2012) Phase transitions in the assembly of multivalent signalling
1207 proteins. *Nature* **483**, 336-340
1208 170. Verkerk, A. J., Pieretti, M., Sutcliffe, J. S., Fu, Y. H., Kuhl, D. P., Pizzuti, A., Reiner,
1209 O., Richards, S., Victoria, M. F., Zhang, F. P., and et al. (1991) Identification of a gene
1210 (FMR-1) containing a CGG repeat coincident with a breakpoint cluster region
1211 exhibiting length variation in fragile X syndrome. *Cell* **65**, 905-914
1212 171. Gohel, D., Sripada, L., Prajapati, P., Singh, K., Roy, M., Kotadia, D., Tassone, F.,
1213 Charlet-Berguerand, N., and Singh, R. (2019) FMRpolyG alters mitochondrial
1214 transcripts level and respiratory chain complex assembly in Fragile X associated
1215 tremor/ataxia syndrome [FXTAS]. *Biochim. Biophys. Acta Mol. Basis Dis.* **1865**,
1216 1379-1388
1217 172. Verma, A. K., Khan, E., Mishra, S. K., and Kumar, A. (2022) Small molecule screening
1218 discovers compounds that reduce FMRpolyG protein aggregates and splicing defect
1219 toxicity in Fragile X-associated tremor/ataxia syndrome. *Mol. Neurobiol.* **59**, 1992-2007
1220 173. Sutton, M. A., and Schuman, E. M. (2006) Dendritic protein synthesis, synaptic
1221 plasticity, and memory. *Cell* **127**, 49-58

174. Bramham, C. R., and Wells, D. G. (2007) Dendritic mRNA: transport, translation and function. *Nat. Rev. Neurosci.* **8**, 776-789

175. Subramanian, M., Rage, F., Tabet, R., Flatter, E., Mandel, J. L., and Moine, H. (2011) G-quadruplex RNA structure as a signal for neurite mRNA targeting. *EMBO Rep* **12**, 697-704

176. Darnell, J. C., Jensen, K. B., Jin, P., Brown, V., Warren, S. T., and Darnell, R. B. (2001) Fragile X mental retardation protein targets G quartet mRNAs important for neuronal function. *Cell* **107**, 489-499

177. Schaeffer, C., Bardoni, B., Mandel, J. L., Ehresmann, B., Ehresmann, C., and Moine, H. (2001) The fragile X mental retardation protein binds specifically to its mRNA via a purine quartet motif. *EMBO J.* **20**, 4803-4813

178. Brown, V., Jin, P., Ceman, S., Darnell, J. C., O'Donnell, W. T., Tenenbaum, S. A., Jin, X., Feng, Y., Wilkinson, K. D., Keene, J. D., Darnell, R. B., and Warren, S. T. (2001) Microarray identification of FMRP-associated brain mRNAs and altered mRNA translational profiles in fragile X syndrome. *Cell* **107**, 477-487

179. Myrick, L. K., Hashimoto, H., Cheng, X., and Warren, S. T. (2015) Human FMRP contains an integral tandem Agenet (Tudor) and KH motif in the amino terminal domain. *Hum. Mol. Genet.* **24**, 1733-1740

180. Vasilyev, N., Polonskaia, A., Darnell, J. C., Darnell, R. B., Patel, D. J., and Serganov, A. (2015) Crystal structure reveals specific recognition of a G-quadruplex RNA by a β-turn in the RGG motif of FMRP. *Proc. Natl. Acad. Sci. U. S. A.* **112**, E5391-5400

181. Westmark, C. J., and Malter, J. S. (2007) FMRP mediates mGluR5-dependent translation of amyloid precursor protein. *PLoS Biol.* **5**, e52

182. Castets, M., Schaeffer, C., Bechara, E., Schenck, A., Khandjian, E. W., Luche, S., Moine, H., Rabilloud, T., Mandel, J. L., and Bardoni, B. (2005) FMRP interferes with the Rac1 pathway and controls actin cytoskeleton dynamics in murine fibroblasts. *Hum. Mol. Genet.* **14**, 835-844

183. Lu, R., Wang, H., Liang, Z., Ku, L., O'Donnell W, T., Li, W., Warren, S. T., and Feng, Y. (2004) The fragile X protein controls microtubule-associated protein 1B translation and microtubule stability in brain neuron development. *Proc. Natl. Acad. Sci. U. S. A.* **101**, 15201-15206

184. Asamitsu, S., Yabuki, Y., Ikenoshita, S., Kawakubo, K., Kawasaki, M., Usuki, S., Nakayama, Y., Adachi, K., Kugoh, H., Ishii, K., Matsuura, T., Nanba, E., Sugiyama, H., Fukunaga, K., and Shioda, N. (2021) CGG repeat RNA G-quadruplexes interact with FMRpolyG to cause neuronal dysfunction in fragile X-related tremor/ataxia syndrome. *Sci. Adv.* **7**, eabd9440

185. Shioda, N., Yabuki, Y., Yamaguchi, K., Onozato, M., Li, Y., Kurosawa, K., Tanabe, H., Okamoto, N., Era, T., Sugiyama, H., Wada, T., and Fukunaga, K. (2018) Targeting G-quadruplex DNA as cognitive function therapy for ATR-X syndrome. *Nat. Med.* **24**, 802-813

186. Wada, T., Suzuki, S., and Shioda, N. (2020) 5-Aminolevulinic acid can ameliorate language dysfunction of patients with ATR-X syndrome. *Congenit. Anom. (Kyoto)* **60**, 147-148

187. Fourier, A., and Quadrio, I. (2022) Proteinopathies associated to repeat expansion disorders. *J. Neural. Transm. (Vienna)* **129**, 173-185

188. Konstantoulea, K., Guerreiro, P., Ramakers, M., Louros, N., Aubrey, L. D., Houben, B., Michiels, E., De Vleeschouwer, M., Lampi, Y., Ribeiro, L. F., de Wit, J., Xue, W. F., Schymkowitz, J., and Rousseau, F. (2022) Heterotypic amyloid β interactions facilitate amyloid assembly and modify amyloid structure. *EMBO J.* **41**, e108591

189. Griner, S. L., Seidler, P., Bowler, J., Murray, K. A., Yang, T. P., Sahay, S., Sawaya, M. R., Cascio, D., Rodriguez, J. A., Philipp, S., Sosna, J., Glabe, C. G., Gonen, T., and Eisenberg, D. S. (2019) Structure-based inhibitors of amyloid β core suggest a common interface with tau. *Elife* **8**, e46924

190. Tetz, G., and Tetz, V. (2021) Bacterial extracellular DNA promotes β-amyloid aggregation. *Microorganisms* **9**, 1301

191. Tetz, G., Pinho, M., Pritzkow, S., Mendez, N., Soto, C., and Tetz, V. (2020) Bacterial DNA promotes tau aggregation. *Sci. Rep.* **10**, 2369

192. Maury, C. P. (2009) Self-propagating β-sheet polypeptide structures as prebiotic informational molecular entities: the amyloid world. *Orig. Life Evol. Biosph.* **39**, 141-150

193. Kappel, K., Zhang, K., Su, Z., Watkins, A. M., Kladwang, W., Li, S., Pintilie, G., Topkar, V. V., Rangan, R., Zheludev, I. N., Yesselman, J. D., Chiu, W., and Das, R. (2020) Accelerated cryo-EM-guided determination of three-dimensional RNA-only structures. *Nat. Methods* **17**, 699-707

194. Sugita, Y., Matsunami, H., Kawaoka, Y., Noda, T., and Wolf, M. (2018) Cryo-EM structure of the Ebola virus nucleoprotein-RNA complex at 3.6 Å resolution. *Nature* **563**, 137-140

195. Pasieka, A., Panek, D., Szalaj, N., Espargaro, A., Wieckowska, A., Malawska, B., Sabate, R., and Bajda, M. (2021) Dual inhibitors of amyloid-β and tau aggregation with amyloid-β disaggregating properties: extended in cellulo, in silico, and kinetic studies of multifunctional anti-Alzheimer's agents. *ACS Chem. Neurosci.* **12**, 2057-2068

196. Okuda, M., Fujita, Y., Hijikuro, I., Wada, M., Uemura, T., Kobayashi, Y., Waku, T., Tanaka, N., Nishimoto, T., Izumi, Y., Kume, T., Akaike, A., Takahashi, T., and Sugimoto, H. (2017) PE859, A novel curcumin derivative, inhibits amyloid-β and tau aggregation, and ameliorates cognitive dysfunction in senescence-accelerated mouse prone 8. *J. Alzheimers Dis.* **59**, 313-328

197. Jiang, X., Lu, H., Li, J., Liu, W., Wu, Q., Xu, Z., Qiao, Q., Zhang, H., Gao, H., and Zhao, Q. (2020) A natural BACE1 and GSK3β dual inhibitor Notopterol effectively ameliorates the cognitive deficits in APP/PS1 Alzheimer's mice by attenuating amyloid-β and tau pathology. *Clin. Transl. Med.* **10**, e50

198. Nan, S., Wang, P., Zhang, Y., and Fan, J. (2021) Epigallocatechin-3-gallate provides protection against Alzheimer's disease-induced learning and memory impairments in rats. *Drug Des. Devel. Ther.* **15**, 2013-2024

199. Ono, K., and Yamada, M. (2006) Antioxidant compounds have potent anti-fibrillogenic and fibril-destabilizing effects for α-synuclein fibrils in vitro. *J. Neurochem.* **97**, 105-115

200. Gabr, M. T., and Peccati, F. (2020) Dual targeting of monomeric tau and α-synuclein aggregation: a new multitarget therapeutic strategy for neurodegeneration. *ACS Chem. Neurosci.* **11**, 2051-2057

201. Ren, X., Zhao, Y., Xue, F., Zheng, Y., Huang, H., Wang, W., Chang, Y., Yang, H., and Zhang, J. (2019) Exosomal DNA aptamer targeting α-synuclein aggregates reduced neuropathological deficits in a mouse Parkinson's disease model. *Mol. Ther. Nucleic Acids* **17**, 726-740

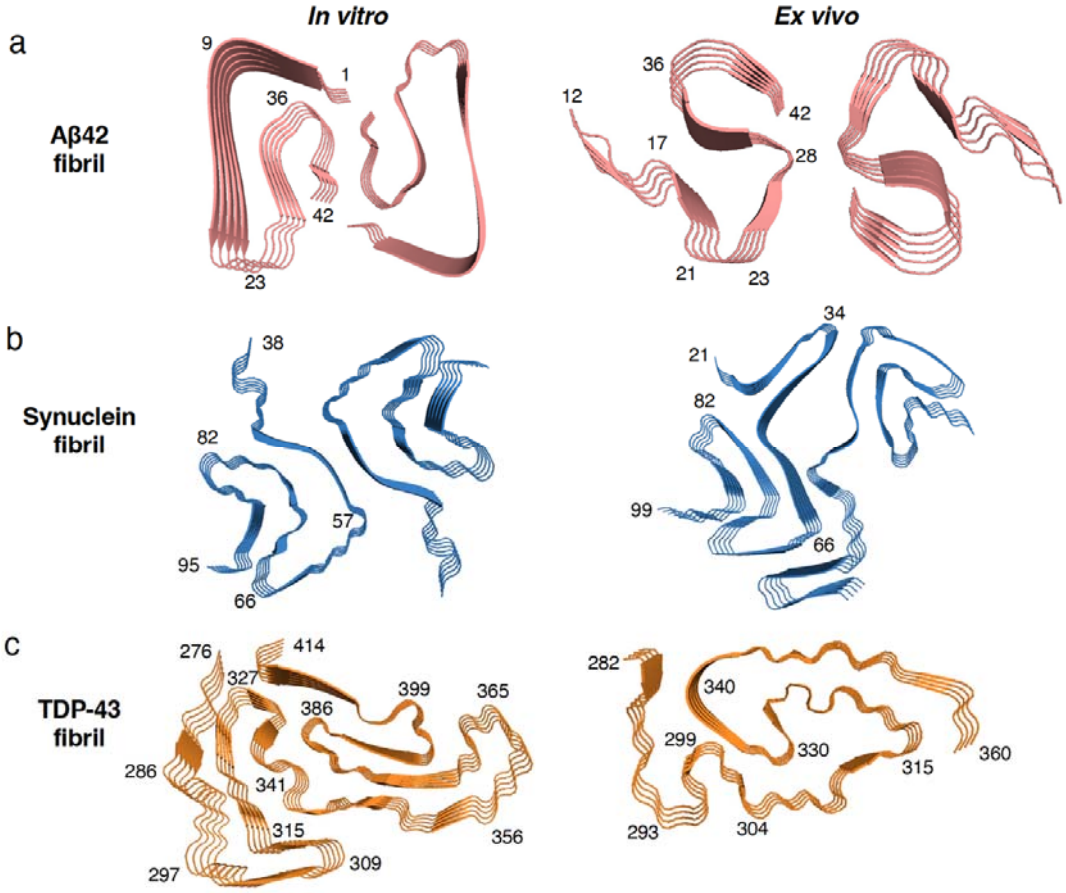


**Fig. 1 Comparison of the *in vitro* and *ex vivo* structures of amyloid fibrils via cryo-EM analysis.** (a) Aβ42 (PDB ID: 5OQV for in vitro, 7Q4M for ex vivo) , (b) αSyn (PDB ID: 6H6B for in vitro, 6XYO for ex vivo), (c) TDP-43 (PDB ID: 7KWZ for in vitro, 7PY2 for ex vivo). PDB, Protein Data Bank. Because ex vivo fibrils formed from Aβ42 and αSyn contained multiple conformers, the representative one is shown.

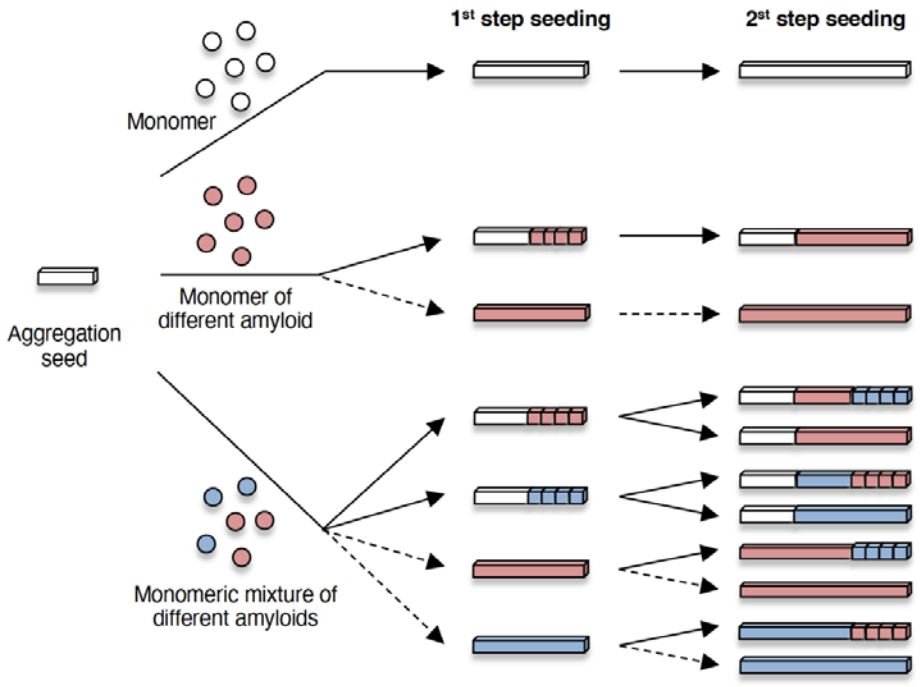


**Fig. 2 Schema of the cross-seeding aggregation model.** The original model proposed by Jarrett and Lansbury (10) for a single amyloidogenic proteins was applied into a combination of multiple amyloids. Various patterns of seeding aggregation depending on the number of amyloids can occur in the presence of seeds as templates of propagation.

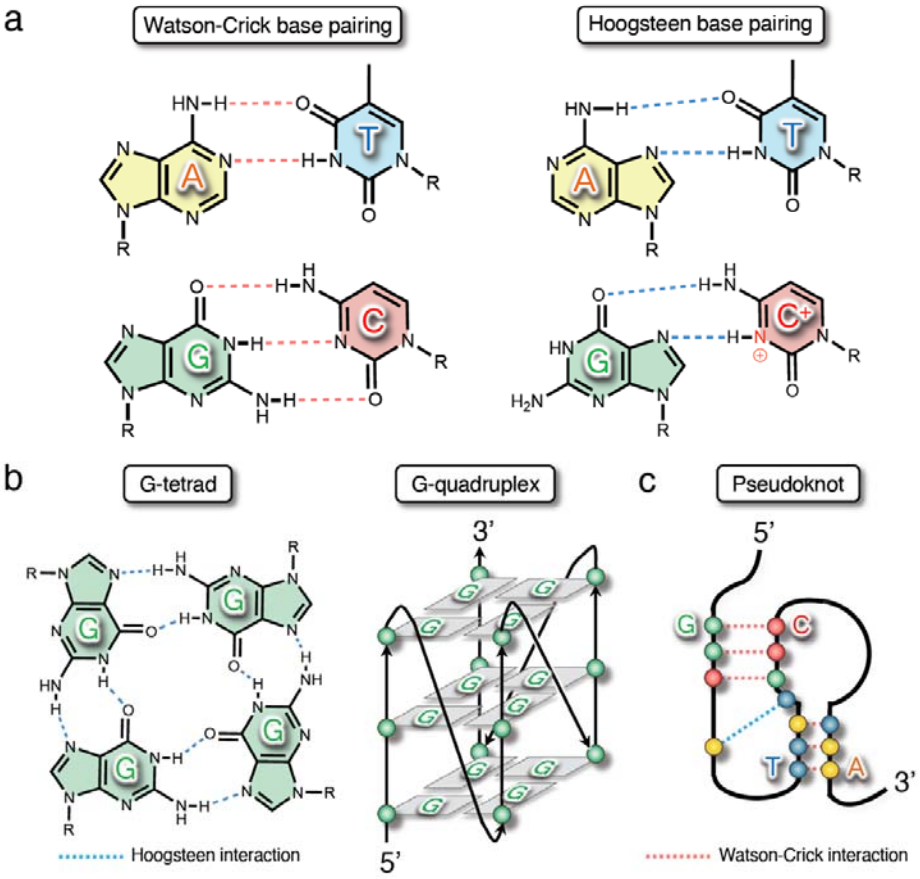


**Fig. 3 Watson-Crick-type and Hoogsteen-type base pairing for natural nucleotides and G-quadruplex formation involved in protein aggregation.** (a) Watson–Crick interactions have three hydrogen bonds between guanine and cytosine and two hydrogen bonds between adenine and thymine. Hoogsteen interactions have two hydrogen bonds between guanine and cytosine and two hydrogen bonds between adenine and thymine, which can be induced by rotating the adenine or guanine by 180° around the glycosidic bond. Although the latter is a minor base pairing of natural nucleotides compared with the former, it allows the formation of triplex and quadruplex structures of DNA or RNA that may contribute to its binding ability with functional proteins and protein aggregation. (b) G-quadruplex structure formed in DNA or RNA by guanine rich sequences induced from Hoogsteen-type interaction. Four guanine bases can form a square planar structure (G-tetrad), and the G-quadruplex is composed of two or more G-tetrads through a stacking process. An intramolecular parallel G-quadruplex that forms three separate G-tetrads stacked 5′ to 3′ with three loops is shown. (c) Pseudoknot structure formed in DNA or RNA by Watson–Crick interaction and Hoogsteen interaction. R denotes the ribose-phosphate backbone.

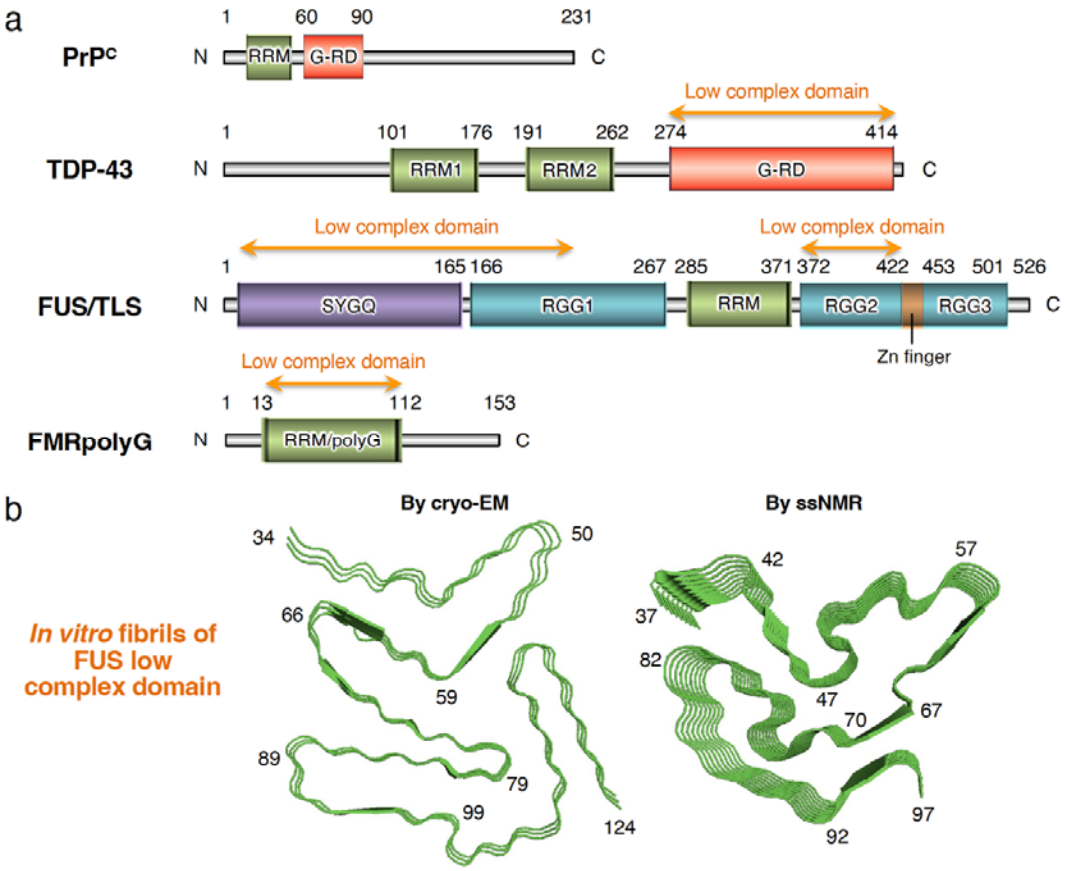


**Fig. 4 Structure and functional domains of RNA-binding proteins that are prone to aggregation.** (a) Prion (231-mer) (87), TDP-43 (414-mer) (123), FUS (526-mer) (148), and FMRpolyG (153-mer) (184) contain several functional domains including an RNA recognition motif (RRM, green) as well as amino acid rich domains such as a glycine rich domain (G, red), serine–tyrosine–glycine–glutamine rich domain (SYGQ, purple), and arginine–glycine–glycine rich domain (RGG, blue). RRM in FMRpolyG is included in a 99-repeated polyglycine (polyG) domain. Low complex domains, indicated by orange double arrows, may play roles in the aggregation and contain putative prion-like domains. (b) Comparison of structures of in vitro fibrils formed from FUS low complex domain according to cryo-EM (PDB ID: 7VQQ) and ssNMR (PDB ID, 5W3N). PDB, Protein Data Bank.

**Table 1. Characteristics of cross-seeding of amyloidogenic proteins.**

| Amyloid | Cross-seeding amyloid | Testing method | Effects | Year | Ref. |
|---|---|---|---|---|---|
| **Aβ – tau** | | | | | |
| Synthetic Aβ42 | Tau (mice) | Aβ-injected P301L-tau Tg mice | NFT↑ | 2001 | (37) |
| Aβ (mice) | Tau (mice) | JNPL3 x Tg2576 mice | NFT↑, Aβ plaques↑ | 2001 | (38) |
| Brain Aβ | Brain tau | AD patients | Aβ-tau complex in NFT | 2006 | (36) |
| **Aβ – αSyn** | | | | | |
| Aβ (mice) | αSyn (mice) | hSYN x J9 Tg mice | Motor deficit↑, αSyn inclusion↑ | 2001 | (44) |
| Brain Aβ | Brain αSyn | AD, PD, DLB patients | Colocalization | 2006 | (45) |
| Brain Aβ | Brain αSyn | DLB patients, Tg mice | Interaction in membrane | 2008 | (47) |
| Fibrillar, oligomeric Aβ40, Aβ42 | Fibrillar, oligomeric αSyn | Th-T, TEM (*in vitro*) | Fibril↑ | 2012 | (48) |
| **Tau – αSyn** | | | | | |
| Tau (mice) | Synthetic αSyn | αSyn-injected P301S-tau Tg mice | Tau inclusion↑ | 2013 | (49) |
| Brain tau | Synthetic αSyn | Injection of αSyn to 5xFAD Tg mice | P-tau and P-αSyn[a] inclusion↑, Aβ plaques↑ | 2020 | (50) |
| **Aβ – IAPP** | | | | | |
| Synthetic Aβ42 | IAPP (mice) | Aβ-injected IAPP Tg mice | Colocalization | 2015 | (56) |
| Oligomeric Aβ42 | Oligomeric IAPP | Th-T, TEM, SDS-PAGE,[b] MTS (*in vitro*) | Fibril↑, oligomer↑, cytotoxicity↑ | 2020 | (55) |
| **αSyn – IAPP** | | | | | |
| Brain αSyn | Brain IAPP | PD, DLB patients | αSyn deposits in pancreatic β cells | 2018 | (57) |
| Synthetic αSyn | IAPP (mice) | αSyn-injected IAPP Tg mice | Amyloid deposits in pancreatic β cells | 2020 | (58) |
| Synthetic αSyn fragment | Synthetic IAPP | Th-T, AFM, MTT (*in vitro*) | Fibril↑, cytotoxicity↓ | 2022 | (59) |

[a]phosphorylated-tau and phosphorylated-αSyn
[b]sodium dodecyl sulfate–polyacrylamide gel electrophoresis

1453 **Table 2. Characteristics of cross-inhibition of amyloidogenic proteins.**

1454

| Amyloid | Cross-seeding amyloid | Testing method | Effects | Year | Ref. |
|---|---|---|---|---|---|
| **TTR – Aβ** | | | | | |
| TTR (mice) | Aβ (mice) | mAb(anti-TTR)-injected Tg2576 mice | Aβ plaques↑, tau phosphorylation↑ | 2004 | (62) |
| TTR (mice) | Aβ (mice) | APPswe/PS1Δ9 x $TTR^{+/-}$ | Insoluble Aβ↑, Aβ plaques↑ | 2007 | (63) |
| Recombinant TTR | Recombinant Aβ40 | Th-T, TEM (*in vitro*) | Nucleation↓ | 2018 | (64) |
| Recombinant TTR | Recombinant Aβ40 | AFM, DLS (*in vitro*) | Nucleation↓, cytotoxicity↓ | 2020 | (65) |
| **TTR – IAPP** | | | | | |
| Recombinant TTR | Synthetic IAPP | Th-T | Nucleation↓, elongation↓ | 2021 | (66) |
| TTR (mice) | Aβ (mice) | HFD[a]-treated $App^{NL-F/NL-F}$ mice | TTR expression↓, Aβ plaques↑ | 2021 | (67) |
| **BRICHOS – Aβ** | | | | | |
| Bri2, Bri3 (recombinant, mice) | Aβ (synthetic, mice, human) | TgAβPParc mice, AD brain, Th-T | Fibril↓, Bri 2, Bri3 bound Aβ (mice, human) | 2018 | (69) |
| Expressed BRICHOS (Drosophila) | Expressed Aβ (Drosophila) | Coexpressed Drosophila | Longevity↑, Aβ plaques↓, locomotor loss↓ | 2014 | (70) |
| Recombinant Bri2, Bri3 | Recombinant Aβ42 | In silico, DLS, SDS-PAGE | Oligomer↓ (Bri2 > Bri3) | 2020 | (74) |
| Recombinant proSP-C | Recombinant Aβ42 | Th-T, TEM, cryo-EM, electrophysiology | Oligomer↓, cytotoxicity (gamma oscillation)↓ | 2015 | (72) |
| Recombinant Bri2 | Recombinant Aβ42 | TEM(3D), SDS-PAGE | Oligomer↓ | 2017 | (73) |
| Expressed proSP-C and Bri2 (Drospphila) | Expressed Aβ (Drosophila) | Coexpressed Drosophila | Longevity↑, locomotor loss↓, impaired eye phenotype↓ | 2016 | (71) |
| **BRICHOS – IAPP** | | | | | |
| Expressed Bri2 (Drosophila) | Expressed IAPP (Drosophila) | Coexpressed Drosophila, Bri2-siRNA-treated EndoC-βH1 cell | Longevity↑, cell death↑ | 2018 | (75) |

1455
1456 [a]high fat diet

1457

**Table 3. Binding characteristics of amyloidogenic proteins and nucleic acids.**[a]

| Amyloid | Nucleic acid | $K_D$ (nM) | Testing method for $K_D$ | Binding region of amyloid | Year | Ref. |
|---|---|---|---|---|---|---|
| **Prion** | | | | | | |
| murine $PrP^C$ ($FL^b$) | plasmid DNA | 250 | light scattering | N.D.[c] | 1999 | (93) |
| murine PrP23-231 | short dsDNA | 25 | light scattering | N- and C-terminal domains | 2001 | (94) |
| hamster PrP23-231 | short dsDNA | 90 | fluorescence polarization | N- and C-terminal domains | 2006 | (98) |
| ovine PrP (FL) | D12 DNA (G4) | 62 | SPR | N- and C-terminal domains | 2013 | (96) |
| Human $PrP^C$ (FL) | tRNA | 1,700 | fluorescence polarization | N- and C-terminal domains | 2018 | (104) |
| Human $PrP^C$ (FL) | Cm47 RNA (pseudoknot) | 1,500 | fluorescence polarization | N- and C-terminal domains | 2018 | (104) |
| **TDP-43** | | | | | | |
| human TDP-43 (FL) | $(UG)_6$ | 27 | EMSA | RRM1 | 2005 | (128) |
| TDP101-261 | RNA34nt-$(UG)_6$ | 5.3 | EMSA | RRM1 | 2013 | (130) |
| human TDP43 (FL) | ssDNA-$(TG)_{12}$ | 90 | FCS[d] | N.D. | 2018 | (132) |
| TDP-43 (RRM1+RRM2) | ssDNA-$(TG)_{12}$ | 51 | ITC | RRM1 loop3, RRM2 pocket around V220 | 2021 | (131) |
| human TDP43 (FL) | RNA14nt | 32 | ITC | N.D. | 2022 | (129) |
| **FUS/TLS** | | | | | | |
| TLS (FL) | ggugRNA25nt | 250 | EMSA | RGG[h] repeats in RRM | 2001 | (158) |
| FUS (FL) | mRNA200nt | 56 | EMSA | RRM, RGG rich domain (Zn finger) | 2015 | (162) |
| TLS/FUS (FL) | $r(UUAGGG)_4$ (G4) | 6.2 | EMSA | RGG rich domain | 2018 | (163) |
| RRM in FUS | hnRNPA2/B1 stem-loop RNA | 9,200 | ITC | RRM, RGG rich domain (Zn finger) | 2019 | (166) |
| TLS/FUS (FL) | PSD-95[i] GQ2 (G4) | 28 | steady-state fluorescence spectroscopy | RGG rich domain | 2020 | (164) |
| FUS (FL) | PSD-95 RNA(G4) | 3.2 | SPR | RGG rich domain | 2021 | (165) |
| **FMRpolyG** | | | | | | |
| FMRpolyG | RNA | N.T.[e] | N.T.[e] | $(CGG)_{99}$ | 2021 | (184) |

[a]Only amyloidogenic proteins whose $K_D$ values were determined are shown when many examples were investigated.
[b]full length
[c]not determined
[d]fluorescence correlation spectroscopy
[e]not tested